

Heavy neutrinos detection in the Next Linear Collider

Ph.D. Thesis

Janusz Gluza

Department of Field Theory and Particle Physics
University of Silesia
Katowice, Poland

January 1997.

Acknowledgments

My special thanks are due to my supervisor Prof. Dr. Marek Zrałek for his constant encouragement and interest. Our conversations were really inspiring and helped me very much.

I also appreciate the financial support from the Polish Committee for Scientific Research, Grants No PB659/P03/95/08 and PB514/P03/96/11.

I'd like to dedicate this work to my Parents, my wife and children Marta and Marek, people who fill my life with happiness.

Contents

1	Introduction	1
2	Light-heavy neutrino mixing angle	6
3	Direct heavy neutrinos production in e^-e^+ collision: $e^-e^+ \rightarrow \nu N$ process	17
3.1	Which Feynman diagrams are the most important?	17
3.2	CP violation effects in the $e^-e^+ \rightarrow N_1N_2$ process (‘see-saw’ model)	22
3.3	‘Non-decoupling’ model and a heavy neutrino in the e^-e^+ collision	31
4	Indirect heavy neutrinos detection in e^-e^- collision: $e^-e^- \rightarrow W^-W^-$ process	40
4.1	CP violation effects in the $e^-e^- \rightarrow W^-W^-$ process (‘see-saw’ model)	41
4.2	‘Non-decoupling model and the $e^-e^- \rightarrow W^-W^-$ process . . .	45
5	Conclusions	50
6	Appendix A. Neutrino mass matrices, their diagonalization and mixing matrices	52
7	Appendix B. Couplings of neutrinos in charged and neutral currents. Couplings of neutrinos with Higgs particles	57
8	Appendix C. Feynman rules for Majorana neutrino interactions	65

1 Introduction

Since the beginning of the standard model's (SM's) construction based on the $SU(3)_C \otimes SU(2)_L \otimes U(1)_Y$ gauge group [1] people realized it had drawbacks¹. However, almost three decades after its birth (and two after Glashow's lecture) the SM seems to be in good shape. It appears that this model describes fundamental electroweak and strong interactions very well and it is hard (till now impossible) to find out something extraordinary, non-standard in nature². The experimental data has become incomparably better, but the theory has remained essentially unmodified.

So, to find out anything beyond the SM, high-energy physicists go generally in one of two directions. First, they are continually improving experimental precision. It's a common belief that with the shrinking error in measurements, some experimental data can finally appear outside its SM value. Second, they use higher and higher energies in experiments. As an illustration of the first approach, let's consider the LEPI program where till the end of 1995 better and better precision of measurements has been achieved. The pay-off for this was, however, unexpected. It appeared that some 'strange' phenomena from the macro-scale world started to be important in par-excellence micro-world experiment as the LEPI is, too. Falling rains, passing trains and the Moon's (and the Sun's) attraction (some people even joke that the LEPI produced the first evidence for gravitational force

¹S. Glashow, one of the founders of this model, said at his Nobel lecture: 'Let me stress that I do not believe that the standard theory will long survive as a correct and complete picture of physics' [2].

²Maybe with two exceptions. The R_b parameter in LEPI at CERN, is about 1.8σ above its SM's value (the situation warmly invited by advocators of theories with supersymmetric extensions of the SM [3]) and the LSND experiment [4] for which the most probable interpretation is that non-vanishing neutrino mass is for the first time observed there.

unification) have influenced and disturbed data collection [5]. So, most probably, in the future higher energies and new machines will be necessary if we are going to investigate fundamental interactions and make any progress in high-energy physics. However, even then, extremely precise measurements from low-energy physics will be useful. For instance, in this Thesis interplay between these two seemingly different approaches is undebated and all the most important conclusions about high energy physics derived here are the result of extraordinary precision obtained in double beta or muon decays among other things.

Because such new experiments are sophisticated nowadays (and expensive), it is necessary to investigate as many phenomena as possible to find out, if these phenomena can be really revealed there. This Thesis is about one such possible phenomenon in the Next Linear Collider (NLC). The NLC collider is one of the many names for the future e^+e^- collider, a machine with a center of mass energy above 200 GeV (LEP II), up to 1500-2000 GeV [6],[7]. The NLC will complement the other future accelerator, the high energy hadron collider LHC at CERN. Together these two machines will provide a coherent program for understanding the SM better and hopefully non-standard, new physics as well.

Many new or un-established ideas such as anomaly couplings, additional (neutral and charged) gauge bosons, excited fermions and Higgs particles can be tested in the NLC collider [8]. Heavy neutrinos are among these ideas and I will deal with this case in this Thesis (for other than ‘NLC’ possibility of heavy neutrino detection - see [9],[10]-[16]).

Although there are three types of massless neutrinos in the SM, almost all extensions of the SM predict more than three massive neutrinos. The last LSND result seems to have claimed, at least partly, this prediction. We know

so far that three known neutrinos are very light with masses [17]

$$m_{\nu_e} \leq 15 \text{ eV}, \quad m_{\nu_\mu} \leq 170 \text{ keV}, \quad m_{\nu_\tau} \leq 24 \text{ MeV}. \quad (1.1)$$

We know from the negative search of new neutral states and from the measurement of Z decay width at the LEPI too, that there are no neutrinos with a standard coupling to Z and mass below $M_Z/2$ [18] or even below M_Z if $BR(Z^0 \rightarrow \nu N) > 3 \cdot 10^{-5}$ [19]. The lack of detection of new neutrino states at the LEPI indicates that if they exist, they will generally have large masses ($\geq M_Z$), attainable in the NLC.

Such masses of heavy neutrinos ($100 \text{ GeV} \leq M_N \leq 0(1) \text{ TeV}$) are natural for a theoretical model based on the $SU(2)_L \otimes SU(2)_R \otimes U(1)_{B-L}$ gauge group [20], the so-called left-right symmetric model (LR). In this model left-handed and right-handed (lepton and quark) fields are treated in the same way: there are 3 left-handed and 3 right-handed doublets (one left-handed and right-handed doublet for each generation). This symmetry causes that apart from three light and known (left-handed) neutrinos we have 3 heavy ($M_N > M_Z$) ones. Their masses are utmost at the level at which the left-right symmetry is broken, e.g. of the order of the right-handed gauge boson mass M_{W_R} . Up-to-date constraints gives $M_{W_R} \geq 406 \text{ GeV}$ [21] (652 GeV [22]), so we can expect to look for heavy neutrinos of the LR model in the NLC collider.

The second easy extension of the SM which includes heavy neutrino particles is the SM supplemented by right-handed singlet neutrino fields (RHS model). Such fields appear naturally in the SO(10) Grand Unified Theory (GUT) in which quarks and leptons are accommodated into one fundamental 16-dimensional representation (3 colours of left- and right-handed u and d quarks plus e_L plus e_R plus ν_L plus N_R). In this GUT model, the natural

mass of such right-handed heavy neutrinos is of the order of the GUT scale ($\sim 10^{15}$ GeV [23]), however much lower neutrino masses ($\sim 0(1)$ TeV) can be possible in principle within the GUT models, too [24].

In this Thesis I will investigate two different processes with heavy neutrinos in the NLC collider for both models mentioned above: direct production of heavy neutrinos by the $e^-e^+ \rightarrow \nu N$ process and their indirect detection by the $e^-e^- \rightarrow W^-W^-$ process. The first process can be realized in Nature both by Majorana and Dirac neutrinos. I will focus here on heavy Majorana neutrinos as a more natural case [25]. The second process can appear only if a neutrino is of the Majorana type (lepton number non-conservation). Other processes with heavy neutrinos in NLC colliders do not seem so promising [26] with the exception of the $e^-\gamma \rightarrow NW^-$ direct production process [27].

This Thesis is organized as follows. Section 2 discusses a possible coupling between light and heavy neutrinos. This parameter is important for processes considered in this Thesis. I also define there two distinctive models: ‘see-saw’ and ‘non-decoupling’ ones for which the magnitude of this parameter can be markedly different. Section 3 discusses the production of heavy neutrinos in an e^-e^+ collision. Possible CP violation effects on the cross section are discussed (‘see-saw’ model) and the most optimistic values of cross section for heavy neutrino production are derived in the framework of the ‘non-decoupling’ model. As the magnitude of this cross section gives hope for a heavy neutrino detection the angular distribution of an electron from a heavy neutrino decay is analysed as a possible heavy neutrino signal in a detector. Section 4 describes the $e^-e^- \rightarrow W^-W^-$ process in which again the CP effects in the ‘see-saw’ model and maximal possible values of cross section (‘non-decoupling’ model) are analysed. Section 5 presents the conclusions of this Thesis.

Three Appendices show how neutrino masses appear both in the RHS and the LR models, describe details about couplings of neutrinos with particles which take part in considered processes and give Feynman rules for Majorana neutrino interactions, used through the Thesis.

2 Light-heavy neutrino mixing angle

In Appendix B I include relevant couplings of neutrino with standard particles which take part in considered $e^-e^+ \rightarrow \nu N$ and $e^-e^- \rightarrow W^-W^-$ processes. The mixing matrix elements K_{Nl} and $\Omega_{N\nu}$ (Eqs.(B.5),(B.28)) which are lepton analog of Cabibbo-Kobayashi-Maskawa matrices in the quark sector are crucial in determining the magnitude of the cross sections. Among them K_{Ne} , coupling of heavy neutrino with electron (positron) is the most important so we have to limit its value as closely as possible.

Generally two approaches can be applied to fix the K_{Ne} parameter. The first is historically known as the ‘see-saw’ model [28] and was established to explain the small masses of known neutrinos. The second (let’s call it the ‘non-decoupling’ model) invokes a symmetry argument to explain the same problem. It appears, however, that apart from neutrino mass explanation other physical variables (as K_{Ne}) can differ significantly in these models. To show generally that it is possible, let’s discuss the ‘toy model’, in which only ‘light’ (ν) and ‘heavy’ (N) neutrinos exist. Let us assume that in the $(\nu, N)^T$ basis the neutrino mass matrix is

$$M = \begin{pmatrix} a & b \\ b & c \end{pmatrix}. \quad (2.1)$$

For simplicity we assume that elements a,b,c are real numbers. The masses and mixing angle are given by

$$m_{1,2} = \frac{1}{2} \left(a + c \mp \sqrt{(a - c)^2 + 4b^2} \right), \quad (2.2)$$

and

$$\sin 2\xi = \frac{2b}{\sqrt{(a - c)^2 + 4b^2}}. \quad (2.3)$$

There are now two ways to predict the light-heavy spectrum of neutrino masses. First is the ‘see-saw’ mechanism where $a=0$ and $c \gg b$ then

$$|m_1| \simeq \frac{b^2}{c}, \quad |m_2| \simeq c \gg m_1, \quad (2.4)$$

and unavoidably (Eq.(2.3))

$$\xi \simeq \frac{b}{c} \ll 1. \quad (2.5)$$

or taking into account relations (2.4)

$$\xi \simeq \sqrt{\frac{|m_1|}{m_2}} \ll 1. \quad (2.6)$$

We can generalize the mass matrix (2.1) to the form as given in the RHS or the LR models (see Appendix A) and then we can expect that the light-heavy neutrino mixing K_{Ne} equals

$$K_{Ne} \sim \frac{\langle m_D \rangle}{\langle M_R \rangle} \quad (2.7)$$

or

$$K_{Ne} \sim \sqrt{\frac{m_{\nu e}}{M_N}}. \quad (2.8)$$

Let’s stick for a moment to an example in which m_D and M_R matrices are taken in the following form

$$m_D = \begin{pmatrix} 1. & 1. & 0.9 \\ 1. & 1. & 0.9 \\ 0.9 & 0.9 & 0.95 \end{pmatrix}, \quad M_R = \begin{pmatrix} 10^2 & 0 & 0 \\ 0 & 10^3 & 0 \\ 0 & 0 & 5000 \end{pmatrix}. \quad (2.9)$$

The neutrino mass matrix M_{diag} which follows (Appendix A) gives a realistic spectrum of neutrino masses ($m_{\nu_e} = 0$ eV, $m_{\nu_\mu} \simeq 16$ μ eV, $m_{\nu_\tau} \simeq 31$ MeV³) - light neutrinos⁴ and ($M_1 = 100$ GeV, $M_2 = 10^3$ GeV, 5000 GeV) - heavy neutrinos.

Mixing matrix U which diagonalize neutrino mass matrix M^ν (Eqs.(A.11), (A.12)) equals

$$U = \begin{pmatrix} .707 & -.38i & -.596i & -.010 & -.001 & .2 \cdot 10^{-3} \\ -.707 & -.38i & -.596i & -.010 & -.001 & .2 \cdot 10^{-3} \\ .3 \cdot 10^{-16} & .84i & -.537i & -.010 & -.001 & .18 \cdot 10^{-3} \\ -.2 \cdot 10^{-16} & .3 \cdot 10^{-14}i & .017i & -1.0 & -.3 \cdot 10^{-5} & .1 \cdot 10^{-6} \\ -.3 \cdot 10^{-16} & .6 \cdot 10^{-15}i & .002i & .3 \cdot 10^{-4} & -1.0 & .1 \cdot 10^{-6} \\ -.5 \cdot 10^{-32} & .9 \cdot 10^{-16}i & .3 \cdot 10^{-3}i & .6 \cdot 10^{-5} & .7 \cdot 10^{-6} & 1.0 \end{pmatrix}.$$

³ This value is too big when we take into account up-to-date data (Eq.(1.1)). However, it makes it possible mention one of neutrinos' experiments which gives an interesting signal lately. An excess of events observed in the KARMEN detector [29] is tentatively interpreted as the decay of 33.9 MeV neutral particle. The identification with ν_τ (SM's, isodoublet) neutrino is rejected by ALEPH limit of 24 MeV [17]. It should be noted, however, that this limit was questioned lately in the context of neutrino mixing scenarios [30]. This value can be easily put down to the ALEPH limit by some play with parameters in matrices m_D, M_R .

⁴We can see that this mass spectrum for light neutrinos is not consistent with cosmological constraints where bound $\sum_{light} m_{\nu_{light}} \leq 23$ eV exists [31]. Masses of the light neutrinos can be reconciled with this agreement in many ways. For instance, we can take $m_D \rightarrow 10^{-3}m_D$ (then interesting mixing angles K_{Ne} will be, however, smaller - in agreement with Eq.(2.7)) or take $m_D = \begin{pmatrix} 1. & 1. & 1. \\ 1. & 1. & 1. \\ 1. & 1. & 1. \cdot 10^{-6} \end{pmatrix}$, $M_R = \begin{pmatrix} M_1 & 10^{-6} & 10^{-6} \\ 10^{-6} & M_2 & 10^{-6} \\ 10^{-6} & 10^{-6} & M_3 \end{pmatrix}$ with relation $\frac{1}{M_1} + \frac{1}{M_2} + \frac{1}{M_3} \simeq 0$ [32] and $M_{1,2,3} \geq 100$ GeV. Then the mixing angles K_{Ne} will be the same as for the matrices (2.9).

From this matrix, other submatrices K and K_R (see Appendix B) can be directly obtained

$$\begin{aligned}
K = & \begin{array}{l} \text{light} \\ \text{neutrinos} \end{array} \rightarrow \begin{array}{c|c|c} \text{e} & \mu & \tau \\ \hline .707 & -.707 & .3 \cdot 10^{-16} \\ -.38 \text{ i} & -.38 \text{ i} & .84 \text{ i} \\ \hline -.596 \text{ i} & -.596 \text{ i} & -.537 \text{ i} \\ \hline \end{array} \\
& \begin{array}{l} \text{heavy} \\ \text{neutrinos} \end{array} \rightarrow \begin{array}{c|c|c} \text{e} & \mu & \tau \\ \hline -.01 & -.01 & -.01 \\ -.001 & -.001 & -.001 \\ \hline .2 \cdot 10^{-3} & .2 \cdot 10^{-3} & .18 \cdot 10^{-3} \\ \hline \end{array} \sim \begin{array}{c} \text{leptons} \\ \left(\begin{array}{c} 0(1) \\ \hline \frac{1}{M_N} \end{array} \right) \end{array},
\end{aligned} \tag{2.10}$$

$$\begin{aligned}
K_R = & \begin{array}{l} \text{light} \\ \text{neutrinos} \end{array} \rightarrow \begin{array}{c|c|c} \text{e} & \mu & \tau \\ \hline -.2 \cdot 10^{-16} & -.3 \cdot 10^{-16} & -.5 \cdot 10^{-32} \\ .3 \cdot 10^{-14} \text{ i} & .6 \cdot 10^{-15} \text{ i} & .9 \cdot 10^{-16} \text{ i} \\ \hline .017 \text{ i} & .002 \text{ i} & .3 \cdot 10^{-3} \text{ i} \\ \hline \end{array} \\
& \begin{array}{l} \text{heavy} \\ \text{neutrinos} \end{array} \rightarrow \begin{array}{c|c|c} \text{e} & \mu & \tau \\ \hline -1.0 & .3 \cdot 10^{-4} & .6 \cdot 10^{-5} \\ -.3 \cdot 10^{-5} & -1.0 & .7 \cdot 10^{-6} \\ \hline .1 \cdot 10^{-6} & .1 \cdot 10^{-6} & 1.0 \\ \hline \end{array} \sim \begin{array}{c} \text{leptons} \\ \left(\begin{array}{c} 0 \\ \hline 0(1) \end{array} \right).
\end{array}
\end{aligned} \tag{2.11}$$

We can see explicitly that we have

$$|K_{Ne}| \sim \frac{1}{M_N}, \tag{2.12}$$

in agreement with our previous estimations (Eq.(2.7)).

Let's note that the values of the m_D matrix elements are justifiable for the LR model (Eqs.(A.25),(A.26)) as

$$\langle m_D \rangle \sim \langle m^l \rangle \sim 0(1) \text{ GeV} \tag{2.13}$$

as long as $h \sim \tilde{h}$. In the RHS model we can choose the same form of the mass matrices m_D and M_R as in Eq.(2.9), so the mixing angle K_{Ne} will be the

same. However, in this model we don't have so strong theoretical motivation for Eq.(2.13) to hold as in the LR model; that is why some people prefer to estimate light-heavy neutrino mixing (K_{Ne}) taking into account relation (2.8) which is based on physical quantities.

Anyhow we must be careful because we can get the wrong relation for K_{Ne} parameter taking into account Eq.(2.8) as our example shows (in this case $K_{Ne} \sim \sqrt{\frac{m\nu_e}{M_N}}$ equals zero exactly, in disagreement with its true value (Eq.(2.10)).

So we have shown that we can find the neutrino mass spectrum in agreement with terrestrial (or cosmological) constraints and to have the mixing angle between light and heavy neutrino in the form given by Eq.(2.12) both for the LR and the RHS models. This is what I call classical 'see-saw' model and I will use this mixing angle in numerical calculations.

Secondly, let us assume that $a \neq 0$ and due to internal symmetry $ac = b^2$, we have

$$\begin{aligned} m_1 &= 0, \\ m_2 &= a + c, \end{aligned} \tag{2.14}$$

and

$$\sin \xi = \frac{2\sqrt{ac}}{a + c}. \tag{2.15}$$

If the symmetry which at the tree level gives the relation $ac = b^2$ is broken we obtain

$$m_1 \neq 0 \ll m_2$$

in the higher order (see e.g. [34]). In this sort of models $\sin 2\xi$ is not connected with the ratio m_1/m_2 and can be large ($\sin 2\xi \simeq 1$) for $a \simeq c$ [11],[25],[35].

So for the ‘non-decoupling’ model the mixing angles are independent parameters not connected to the neutrino masses and are only bound by existing experimental data. Constraints come from:

(i) Low energy experiments (e.g. lepton universality, the μ decay) and the LEPI give also information about heavy neutrinos with masses above M_Z . The reason is that due to unitarity properties of the U matrix (Eq.(A.11)), the nonzero mixing matrix elements K_{Ne} (Eqs.(B.5),(B.28)) slightly reduce the couplings of light neutrinos from their SM values thus affecting all processes including these particles [36] (in the SM matrix U can be taken as I and then matrix K in Eq. (B.3) equals I, too). The up-to-date limit for the RHS model is [15]

$$\sum_{N(\text{heavy})} K_{Ne}^2 \leq \kappa^2 = 0.0054. \quad (2.16)$$

Practically the same limit exists for the LR model ([37]).

(ii) The lack of signal of neutrinoless double- β decay $(\beta\beta)_{0\nu}$ gives the bound for light neutrinos

$$\left| \sum_{\nu(\text{light})} K_{\nu e}^2 m_\nu \right| < \kappa_{\text{light}}^2 \quad (2.17)$$

where $\kappa_{\text{light}}^2 < 0.65$ eV [38].

(iii) From the $(\beta\beta)_{0\nu}$ process it is also possible to get the bound for heavy neutrinos⁵

$$\left| \sum_{N(\text{heavy})} K_{Ne}^2 \frac{1}{M_N} \right| < \omega^2. \quad (2.18)$$

⁵This bound can be obtained when more than one nuclei is considered. Then because nuclear matrix elements differ from nucleus to nucleus, possible cancelations in amplitude between light and heavy neutrinos’ contributions can not appear in all nuclei simultaneously [39].

The up-to-date value is $\omega^2 < (2 - 2.8) \cdot 10^{-5} \text{ TeV}^{-1}$ for the RHS model [40] and similarly for the LR model [41] ⁶.

The last constraint which I use to fix K_{Ne} comes from the fact that the mass term for the left-handed neutrinos is absent. Then (Eqs.(A.9), (A.11),(A.12))

(iv)

$$\sum_{\nu(light)} K_{\nu e}^2 m_\nu + \sum_{N(heavy)} K_{Ne}^2 M_N = M_L \equiv 0. \quad (2.19)$$

This fact confronted with Eq.(2.17) gives

$$\left| \sum_{N(heavy)} K_{Ne}^2 M_N \right| < \kappa_{light}^2. \quad (2.20)$$

This relation includes an interesting information. To get meaningful values of cross sections for the studied processes as large as possible values of K_{Ne} are needed. As κ_{light}^2 is very small the only possibility to reconcile these two facts is to assume that some K_{Ne} matrix elements are complex numbers. If CP symmetry is conserved then neutrinos with purely complex K_{Ne} numbers have opposite η_{CP} parities to neutrinos with real ones [23]. Relation (2.19) was important to get this conclusion. However, we know that Majorana neutrinos get mass through radiative corrections [34], [44] and consequently Eq.(2.19) must be modified

$$\sum_{\nu(light)} K_{\nu e}^2 m_\nu + \sum_{N(heavy)} K_{Ne}^2 M_N = M_L^r \quad (2.21)$$

⁶Some people claim [42] that this value is too strict and can be loosen by a factor ~ 40 . It does not change, however, any other conclusions given there quantitatively. The most important for our discussion is that such bound can be derived from experimental data (the situation when the relation (2.18) is not taken into account were considered in [43].

We don't know in principle how large M_L^r can be. In what follows I will hold this general formula with M_L^r .

Taking into account relations (2.16)-(2.21) the largest possible K_{Ne} depends on the number of right-handed neutrinos n_R ($n_R = 3$ in the LR model)

- $n_R = 1$ or all heavy neutrinos with the same CP parities

In this case very restrictive constraint results from Eqs.(2.17),(2.21)

$$\left| M_L^r - \sum_N K_{Ne}^2 M_N \right| < \kappa_{light}^2. \quad (2.22)$$

For $M_L^r \simeq 0$ mixing angle K_{Ne} is extremely small. Another strict constraint follows from Eq.(2.18)

$$| K_{Ne}^2 | < \omega^2 M. \quad (2.23)$$

- $n_R = 2$

In agreement with the previous discussion we assume that both heavy neutrinos have opposite CP parities. Let us take $\eta_{CP}(N_1) = -\eta_{CP}(N_2) = i$. If we denote $K_{N_1e} = x_1$, $K_{N_2e} = ix_2$, $m_1 = M$, $m_2 = AM$ ($A > 1$) then from Eqs.(2.16)-(2.18),(2.21) we get

$$x_1^2 + x_2^2 \leq \kappa^2 \quad (2.24)$$

$$\left| \frac{M_L^r}{M} - x_1^2 + Ax_2^2 \right| \leq \frac{\kappa_{light}^2}{M} \quad (2.25)$$

$$\left| x_1^2 - \frac{x_2^2}{A} \right| \leq \omega^2 M. \quad (2.26)$$

In Eq.(2.25) $\delta \equiv \frac{\kappa_{light}^2}{M}$ is very small for $M > 100$ GeV ($\delta < 10^{-11}$). Since we want to have values of x_1^2 and/or x_2^2 mixing angles as large as possible then $\delta \ll x_1^2, Ax_2^2$, and δ parameter can be practically neglected. It gives

$$\left(\frac{M_L^r}{M} \equiv \Delta^r\right)$$

$$x_1^2 = \Delta^r + Ax_2^2 \quad (2.27)$$

and from inequalities (2.24) and (2.26) we get that masses and mixing angles of heavy neutrinos with electron must satisfy the following relations

$$x_1^2 \leq A \frac{\kappa^2 - \Delta^r}{A+1} + \Delta^r \quad \text{and} \quad x_1^2 \leq \frac{A^2 \omega^2 M - \Delta^r}{A^2 - 1} \quad (2.28)$$

and

$$x_2^2 \leq \frac{\kappa^2 - \Delta^r}{A+1} \quad \text{and} \quad x_2^2 \leq \frac{A}{A^2 - 1} (\omega^2 M - \Delta^r). \quad (2.29)$$

As for masses $0.1 \text{ TeV} < M < 1 \text{ TeV}$, $\kappa^2 \gg \omega^2 M$, the second inequalities are usually stronger. The only possible way to get large x_1^2 is to assume that $A \rightarrow 1$. We can derive some information about M_L^r , too. From Eqs.(2.28),(2.29) we have $\Delta^r \leq \omega^2 M$, so for given value ω^2 we have

$$M_L^r \leq 10 \text{ MeV}. \quad (2.30)$$

However, for $M \geq 1 \text{ TeV}$ restrictions weaken very fast. The largest possible values of the mixing matrix elements are ($A \rightarrow 1$)

$$\begin{aligned} K_{N_1 e}^2 &\rightarrow \frac{\kappa^2}{2}, \\ K_{N_2 e}^2 &\rightarrow \frac{\kappa^2}{2}. \end{aligned} \quad (2.31)$$

Neutrinos with those mixing angles have opposite CP parities, so Dirac neutrino is realized there.

- $n_R = 3$

Let's assume that $\eta_{CP}(N_1) = \eta_{CP}(N_2) = -\eta_{CP}(N_3) = i$. If we denote $K_{N_1 e} = x_1$, $K_{N_2 e} = x_2$, $K_{N_3 e} = ix_3$ and $m_1 = M$, $m_2 = AM$, $m_3 = BM$,

then relations (2.16)–(2.21) give a set of inequalities. I consider the more interesting case $A > B$ (for $A < B$ the mixing parameters are much smaller) in which the following inequalities are satisfied

$$x_2^2 \leq -x_1^2 \frac{1+B}{A+B} + \left(\kappa^2 + \frac{\Delta^r}{B} \right) \frac{B}{A+B}, \quad (2.32)$$

$$x_2^2 \geq x_1^2 \frac{B^2-1}{A^2-B^2} A - \left(\omega^2 M - \frac{\Delta^r}{B^2} \right) \frac{AB^2}{A^2-B^2}, \quad (2.33)$$

and

$$x_2^2 \leq x_1^2 \frac{B^2-1}{A^2-B^2} A + \left(\omega^2 M + \frac{\Delta^r}{B^2} \right) \frac{AB^2}{A^2-B^2}. \quad (2.34)$$

x_3^2 can be found from the relation

$$x_3^2 = \frac{1}{B} (x_1^2 + Ax_2^2 - \Delta^r). \quad (2.35)$$

From inequalities (2.32)–(2.34) we can find a region in the (x_1^2, x_2^2) plane of still acceptable mixing parameters. The region (which is schematically shown in Fig. 1) depends on the chosen values of M , A and B .

Maximal values of mixing matrix elements are ($A \rightarrow \infty$)

$$\begin{aligned} x_1^2 &\rightarrow \frac{\kappa^2 + BM\omega^2}{1+B} \\ x_2^2 &\rightarrow 0 \\ x_3^2 &\rightarrow \frac{B\kappa^2 - BM\omega^2}{1+B}. \end{aligned} \quad (2.36)$$

We can see that in this case a heavier neutrino can have a larger mixing angle than the lightest one.

Let's stress once more that quantitatively restrictions given in Eqs.(2.32)–(2.35) are true both for the LR and the RHS models as κ^2 , and ω^2 are practically the same in both models.

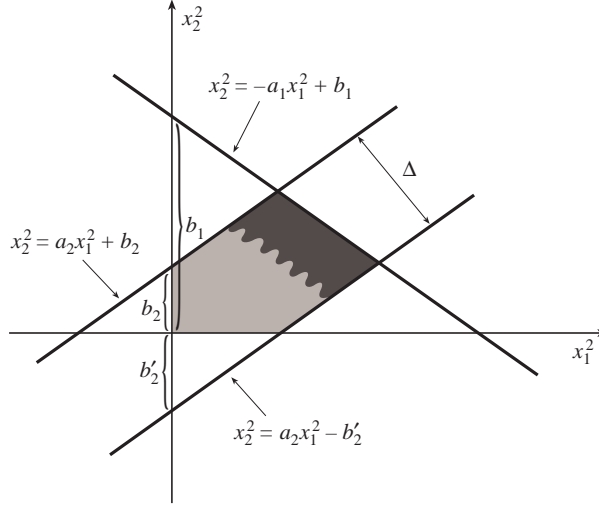


Fig.1. Sketch of the region in $x_1^2 - x_2^2$ plane of still experimentally acceptable mixing parameters. I use the following denotations (see Eqs. (2.32)-(2.34) in the text)

$$a_1 = \frac{1+B}{A+B}, \quad b_1 = \left(\kappa^2 + \frac{\Delta^r}{B}\right) \frac{B}{A+B}, \quad a_2 = A \frac{B^2-1}{A^2-B^2}$$

$$b_2 = \left(\omega^2 M - \frac{\Delta^r}{B^2}\right) \frac{AB^2}{A^2-B^2}, \quad b'_2 = \left(\omega^2 M + \frac{\Delta^r}{B^2}\right) \frac{AB^2}{A^2-B^2}$$

For masses $M < 1$ TeV, $b_2 \sim b'_2 \ll 1$ and the region is very narrow ($\Delta \rightarrow 0$). The more shadowed region is the place where the mixing angles are the largest.

3 Direct heavy neutrinos production in e^-e^+ collision: $e^-e^+ \rightarrow \nu N$ process

3.1 Which Feynman diagrams are the most important?

At the tree level the $e^-e^+ \rightarrow N_a N_b$ process proceed through the following Feynman diagrams (Fig.2).

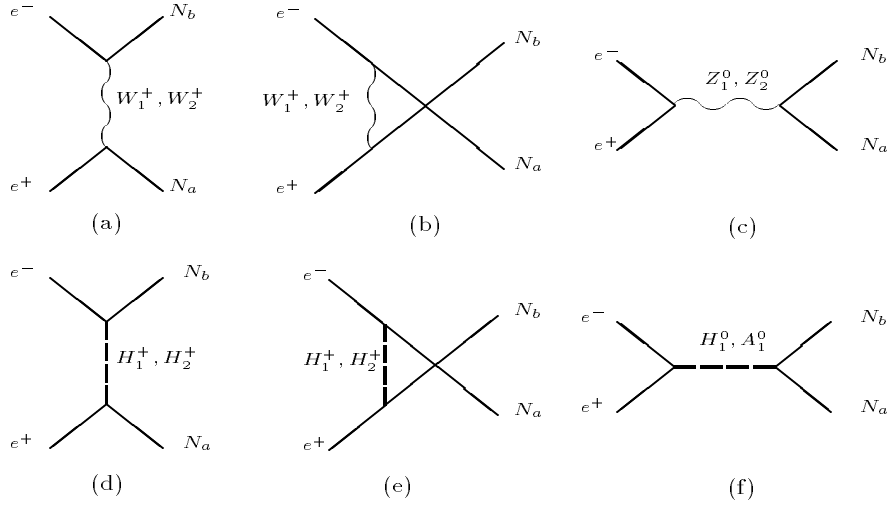


Fig.2 $e^-e^+ \rightarrow N_a N_b$ process at the tree level in the framework of the LR model.

N_a and N_b stand for any neutrinos - light or heavy. Denotations are given for the LR model where we have two pairs of charged and neutral gauge bosons and couple of Higgs particles (only Higgs particles with nonzero couplings to electrons are depicted there - see Appendix B for details). In the framework of the RHS model only two first diagrams contribute (with only one charged gauge boson $W_1^- \equiv W^-$). I will consider Majorana neutrinos, so crossing diagrams are taking into account.

e^+e^-	$\rightarrow \nu N$	$\rightarrow NN$
W_1	$\sim 0.2\%$	$\sim 99.5\%$
Z_1	$\sim 97.5\%$	$\sim 99.5\%$
W_2	$\sim 99.9\%$	$\sim 2\%$
Z_2	$\sim 99.9\%$	$\sim 99.2\%$

Table 1: The contributions of different diagrams with $W_{1,2}$ and $Z_{1,2}$ exchange to the total cross section. The numbers in the table present the part of σ_{total} after removing corresponding diagrams.

The t- and u-channels are the most important for this process with the W_1 exchange. Other, like $Z_{1(2)}$ contributions, are negligible because of off-peak energies ($\sqrt{s} \gg M_{Z_1}$) and a large mass of additional gauge boson Z_2 ($\sqrt{s} \ll M_{Z_2}$) - see Eq.(B.16). The W_2 gauge boson couples with an electron predominantly by the right-handed currents (see Eqs.(B.18) and (B.21)). Large mass of W_2 decide, however, about smallness of the W_2 contribution to the process. To be specific, results for $\sqrt{s} = 500$ GeV collider are summarized in Table 1 where the case of two heavy neutrinos production is included, too (with contribution dominated by the W_2 exchange). That is why results for the LR and the RHS models are practically the same for the single heavy neutrino production in the e^-e^+ collision.

Apart from additional gauge bosons in the LR model additional contributions to this process come from Higgs particles' exchange (Fig.2). I use the unitary gauge so diagrams with Goldstone particles exchange are not taken into account. How much can they change results? The precise values of all couplings are presented in Appendix B. In the approximation used

here ($v_R \gg y$, $m_e \simeq 0$) (Eq.(B.29)) only two neutral Higgses couple in the s channel. The lightest Higgs particle H_0^0 (equivalent of the SM's one) couples to the e^-e^+ proportionally to the electron mass and its effect is negligible in the energy range which I consider (see Eq.(B.35)). The influence of two charged $H_{1,2}^+$ and two neutral (H_1^0, A_1^0) Higgs particles is not obvious. At first sight their coupling, even to the light leptons ($e^-e^+, e\nu$), can be large as there are terms in the vertex proportional to heavy neutrinos mass. They are, however, multiplied by the mixing matrices which can have small terms so the total effect needs precise analysis.

For $M_{W_1} = 80$ GeV and $M_{W_2} = 1600$ GeV [45] we can find (Eqs.(B.15-16)) $y \simeq 250$ GeV, $v_R \simeq 3500$ GeV and then for $\epsilon = 0$ all Higgs boson masses are of 2.5 TeV order (Eq.(B.30))

$$M_{H_1^\pm} \simeq M_{H_2^\pm} \simeq M_{H_1^0} \simeq M_{A_1^0} \simeq 2450 \text{ GeV}. \quad (3.1)$$

For the neutral Higgs bosons H_1^0 and A_1^0 the masses of order 2.5 TeV are not large enough to reduce the $\bar{K}^0 - K^0$ transition. To generate proper mass splitting in $\bar{K}^0 - K^0$ system it was found that masses of neutral Higgs particles must be above 10 TeV. Otherwise these particles could have caused that flavour changing neutral currents (FCNC) were too large [46],[47].

There are two ways of obtaining such large masses of neutral Higgs bosons. Firstly we can assume that some parameters which are present in Higgs potential are very large (greater than 1). Then minimalization of the Higgs potential can give larger masses of Higgs particles [48].

Secondly, we can avoid the fine tuning problem for the Higgs parameters mentioned above by taking the same VEV $\kappa_1 \simeq \kappa_2$, so then $\epsilon \simeq 1$ (Eq.(B.30)) and the masses $M_{H_1^0}, M_{A_1^0}$ and $M_{H_2^\pm}$ are much greater than $\frac{1}{2}v_R^2$, so greater than 10 TeV.

In the first case the presence of large masses in the propagator causes that the total contribution of the H_1^0 and A_1^0 exchange in the s channel is very small. When $\epsilon \rightarrow 1$, the couplings of neutral Higgses H_1^0 and A_1^0 to leptons become stronger (see Eqs.(B.34)-(B.36)) and compensate the influence of the propagator. The total effect depends on the additional vertex contributions given in Eqs.(B.35) and (B.36). I have calculated numerically the factors of the type

$$(K^\dagger M_{diag}^\nu K_R)_{ee} \ , \ (K m_l^{diag} K_R^\dagger)_{ab} \ , \ (\Omega M_{diag}^\nu)_{ab} \quad (3.2)$$

which are present in those couplings for different values of the heavy neutrino masses. K, K_R, Ω and M_{diag}^ν are taken as discussed in Section 2 (Eqs.(2.9)-(2.11),(B.28)). Then the factors are of the same order independently of the neutrino masses. It is caused by the fact that for larger neutrino masses the appropriate mixing matrix elements are smaller. I have checked that the influence of the scalar H_1^0 and pseudoscalar A_1^0 exchange diagrams on the total cross section is completely negligible for considered energy range. I have checked also the contribution of the charged Higgs bosons exchange in the t-u channels. In Table 2 the ratios of cross sections with only gauge bosons (σ_{gauge}) or Higgs particles (σ_{Higgs}) to σ_{total} in which all Feynman diagrams are taken into account are presented. We can see that Higgses have no meaning for heavy Majorana neutrino production. For $\nu_\mu N$ and $\nu_\tau N$ neutrino production the Higgs exchange mechanism gives only the contribution of the order of 10^{-4} . Moreover, these results are not sensitive to the ϵ factor. The Feynman diagram with H_1^+ exchange (which is the most important) is not sensitive to this factor at all (Eqs.(B.30),(B.31)). The H_2^+ exchange diagram is sensitive to this factor and the contribution to the total cross section increases with increasing ϵ (Eqs.(B.32),(B.33)), but as the propagator for this particle is sensitive to this factor, too (Eq.(B.30)), the increase is rather

e^-e^+	$\sigma_{gauge}/\sigma_{total}$	$\sigma_{Higgs}/\sigma_{total}$
$\rightarrow \nu_e N(100)$	$\simeq 100\%$	$\simeq .0001\%$
$\rightarrow \nu_\mu N(100)$	$\simeq 100\%$	$\simeq .01\%$
$\rightarrow \nu_\tau N(100)$	$\simeq 100\%$	$\simeq .01\%$

Table 2: The contribution of the gauge and Higgs bosons to the total cross section for LEP II energy.

small and even for $\epsilon = 1$ does not predominate the H_1^+ contribution. The result is shown in Fig.3 for the $e^-e^+ \rightarrow \nu_\tau N$ ($M_N = 100$ GeV) process.

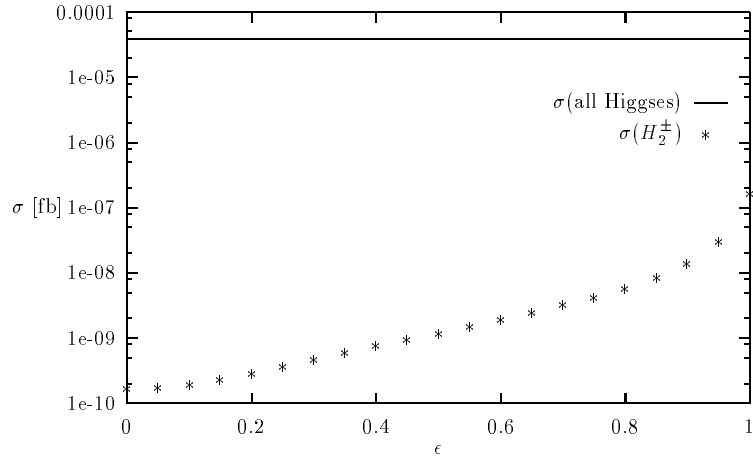


Fig.3. The ϵ dependence for $\sigma[e^-e^+ \rightarrow \nu_\tau N(100)]$ cross section given by all physical Higgs boson exchange (solid line) and only by H_2^+ Higgs boson exchange (asterisk line) for LEP II energy.

To sum up, two first diagrams from Fig.2 give the largest contribution to the single heavy neutrino production process (W_1 exchange) and to the pair of heavy neutrino production process (W_2 exchange). Helicity amplitudes for these diagrams are gathered in Eqs. (3.3)-(3.5) (full details with all Feynman

diagrams Fig.2 (a)-(f) are given in [48]) where $\sigma, \bar{\sigma}, \lambda_{1,2}$ denote helicities of electron, positron and two heavy neutrinos respectively, $\beta_{1,2} = \frac{q}{E_{1,2}}$ are kinematical factors with q - momentum, $E_{1,2}$ - energy of produced neutrinos in CM frame and index $i=1,2$ describes two charged gauge bosons

$$-iM(\sigma, \bar{\sigma}; \lambda, \bar{\lambda}) \propto \frac{A_1^{t_i}}{t - M_{W_i}^2} - \frac{A_1^{u_i}}{u - M_{W_i}^2}, \quad (3.3)$$

$$\begin{aligned} A_1^{t_i}(\sigma, \bar{\sigma}; \lambda_1, \lambda_2) &= (A_L^i)_{1e}^* (A_L^i)_{2e} \delta_{\Delta\sigma, -1} \sqrt{(1 - 2\lambda_1\beta_1)(1 + 2\lambda_2\beta_2)} \\ &+ (A_R^i)_{1e}^* (A_R^i)_{2e} \delta_{\Delta\sigma, +1} \sqrt{(1 + 2\lambda_1\beta_1)(1 - 2\lambda_2\beta_2)}, \end{aligned} \quad (3.4)$$

$$\begin{aligned} A_1^{u_i}(\sigma, \bar{\sigma}; \lambda_1, \lambda_2) &= A_1^{t_i*}(\lambda_1 \longleftrightarrow \lambda_2, \beta_1 \longleftrightarrow \beta_2) \\ &= (A_L^i)_{1e} (A_L^i)_{2e}^* \delta_{\Delta\sigma, -1} \sqrt{(1 - 2\lambda_2\beta_2)(1 + 2\lambda_1\beta_1)} \\ &+ (A_R^i)_{1e} (A_R^i)_{2e}^* \delta_{\Delta\sigma, +1} \sqrt{(1 + 2\lambda_2\beta_2)(1 - 2\lambda_1\beta_1)}, \end{aligned} \quad (3.5)$$

Factors $A_{L,R}^i$ are defined in Eq.(B.21). As we can see these factors in principle are not real and their complex phases are connected with CP violation effects in the lepton sector. As their complexity caused destructive or constructive interferences among different terms in Eqs.(3.3)-(3.5) it is worth to investigate the influence of CP phases on the considered reaction.

3.2 CP violation effects in the $e^-e^+ \rightarrow N_1N_2$ process ('see-saw' model)

CP violation have been observed until now only as a small effect in the $K^0 - \bar{K}^0$ system (quark sector). Smallness of this effect is understood in the framework of the SM. Physical quantities must be independent of the choice of weak basis so only weak basis invariants enter in a measurable quantity.

It can be shown that for 3 families there is only one independent invariant which can be built of quark mass matrices M_u, M_d [49]

$$\begin{aligned} \{\text{weak invariant}\} = & -2i(m_t^2 - m_c^2)(m_t^2 - m_u^2)(m_c^2 - m_u^2)(m_b^2 - m_s^2) \\ & (m_b^2 - m_d^2)(m_s^2 - m_d^2) \text{Im}(V_{cd}V_{ub}V_{cb}^*V_{ud}^*) \end{aligned} \quad (3.6)$$

where V_{ij} are elements of the Cabibbo-Kobayashi-Maskawa mixing matrix. Because quark masses are non-degenerate then in the SM all CP violating effects are proportional to

$$\delta_{KM} = \text{Im}(V_{cd}V_{ub}V_{cb}^*V_{ud}^*). \quad (3.7)$$

Using the unitarity of the CKM matrix we can write

$$|\delta_{KM}| = |\text{Im}(V_{cd}V_{ub}V_{cb}^*V_{ud}^*)| \quad (3.8)$$

and substituting experimental values we have

$$|\delta_{KM}| < 10^{-4}. \quad (3.9)$$

This tiny quantity is responsible for CP violation effect in $K^0 - \bar{K}^0$ system.

No CP violation has been observed in the lepton sector. This can be related to the smallness of the masses of the known neutrinos. Heavy Majorana neutrinos can potentially change this situation.

CP violation effects can be caused by complex phases in the mixing matrices K and K_R . However not all phases in the mixing matrices are CP violating. Some of them can be eliminated by redefinition the fermion fields. For instance, in the quark sector of the SM, six phases which define 3×3 unitary mixing matrix reduce to one phase after appropriate fermion fields redefinition [50]. Let's check how does it work for considered the LR model.

The relevant parts of the model's Lagrangian for studying the CP properties are the charged-current interaction and the lepton mass Lagrangian. They are given by (weak basis)

$$L_{CC} = \frac{g}{\sqrt{2}} \left(\bar{\nu}_L \gamma^\mu l_L W_{L\mu}^+ + \bar{\nu}_R \gamma^\mu l_R W_{R\mu}^+ \right) + h.c. \quad (3.10)$$

and (Eqs.(A.21),(A.24-26))

$$L_{mass} = -\frac{1}{2} (\bar{n}_L^c M_\nu n_R + \bar{n}_R M_\nu^* n_L^c) - (\bar{l}_L m^l l_R + \bar{l}_R m^{l\dagger} l_L) \quad (3.11)$$

where n_R is a six-dimensional vector of the neutrino fields

$$\begin{aligned} n_R &= \begin{pmatrix} \nu_R^c \\ \nu_R \end{pmatrix}, \quad \nu_R^c = i\gamma^2 \nu_L^*, \\ n_L &= \begin{pmatrix} \nu_L \\ \nu_L^c \end{pmatrix}, \quad \nu_L^c = i\gamma^2 \nu_R^*. \end{aligned} \quad (3.12)$$

The most general CP transformation which leaves the gauge interaction (3.10) invariant is [51]

$$\begin{aligned} l_L &\rightarrow V_L C l_L^*, \quad \nu_L \rightarrow V_L C \nu_L^*, \\ l_R &\rightarrow V_R C l_R^*, \quad \nu_R \rightarrow V_R C \nu_R^*. \end{aligned} \quad (3.13)$$

where $V_{L,R}$ are 3×3 unitary matrices acting in lepton flavour space and C is the Dirac charge conjugation matrix. For the full Lagrangian to be invariant under (3.13) the lepton mass matrices m_D, M_R and m^l have to satisfy the conditions

$$\begin{aligned} V_L^\dagger m_D V_R &= m_D^*, \\ V_R^T M_R V_R &= M_R^*, \end{aligned} \quad (3.14)$$

and

$$V_L^\dagger m^l V_R = (m^l)^*. \quad (3.15)$$

The relations expressed by Eqs.(3.14) and (3.15) are weak-basis independent and constitute necessary and sufficient condition for CP invariance. It means that if for given matrices m_D , M_R and m^l , there exist two unitary matrices V_L and V_R such that relations (3.14),(3.15) hold then the model is CP invariant and, on the other hand, if CP is the symmetry of the model then such matrices V_L and V_R exist. The most convenient basis for studying CP symmetry is the weak basis in which charged lepton mass matrix m^l is real, positive and diagonal [52]

$$m^l = \text{diag}[m_e, m_\mu, m_\tau]. \quad (3.16)$$

Then for non-degenerate, non-vanishing $m_e \neq m_\mu \neq m_\tau$ Eq.(3.14) and (3.15) imply that matrices $V_{L,R}$ are diagonal and equal

$$V_L = V_R = \text{diag}[e^{i\delta_1}, e^{i\delta_2}, e^{i\delta_3}]. \quad (3.17)$$

From Eqs.(3.14) and (3.15) then it follows that the model has CP symmetry if and only if the matrices m_D and M_R have the elements

$$\begin{aligned} (m_D)_{ij} &= |(m_D)_{ij}| e^{+\frac{i}{2}(\delta_i - \delta_j)}, \\ (M_R)_{ij} &= |(M_R)_{ij}| e^{-\frac{i}{2}(\delta_i + \delta_j)} \end{aligned} \quad (3.18)$$

in the basis where m^l is diagonal. Altogether we have six CP-violating phases ($\frac{n(n+1)}{2}$ = for symmetric M_R plus $\frac{n(n-1)}{2}$ for hermitian m_D give totally n^2 phases minus n phases connected with fields redefinition) which can be written in the form

$$\begin{aligned} M_R &= \begin{pmatrix} M_{11}e^{i\alpha_1} & M_{12} & M_{13} \\ M_{12} & M_{22}e^{i\alpha_2} & M_{23} \\ M_{13} & M_{23} & M_{33}e^{i\alpha_3} \end{pmatrix}, \\ m_D &= \begin{pmatrix} m_{11} & m_{12}e^{i\beta_1} & m_{13}e^{i\beta_2} \\ m_{12}e^{i\beta_1} & m_{22} & m_{23}e^{i\beta_3} \\ m_{13}e^{i\beta_2} & m_{23}e^{i\beta_3} & m_{33} \end{pmatrix}. \end{aligned}$$

For energies much bigger than the masses of neutrinos N_1 and N_2 ($\sqrt{s} \gg 0(1)$ TeV) or when $\sqrt{s} \sim 0(1)$ TeV but with at least one light neutrino, the t channel predominantly contributes to the $M(-+; -+)$ amplitude (left-handed current) and $M(+--; +-)$ one (right-handed current) and the u channel gives contributions to $M(-+; +-)$ and $M(+--; -+)$ amplitudes (see Eqs.(3.4)-(3.5)). We can see that in these cases there is no interference between t and u channels.

For the energy just above the production threshold there is no helicity suppression mechanism for two heavy neutrino production process $e^-e^+ \rightarrow N_1N_2$ (Eqs.(3.4)-(3.5)) and final neutrinos with all helicity states can be produced by each channel diagram. These are the best conditions for observing the CP violation effects because in this case t and u channels contribute to the same helicity states. As heavy neutrinos predominantly couple to W_2 gauge bosons (see matrix U (Eq.(2.11) with $(K_R)_{N_4e} = 1$ and Eq.(B.21)), the diagrams with W_2 (right-handed currents) are the most interesting (that is the reason why we don't consider results for the RHS case at all as they are small in comparison to the LR model ones).

Another question is in what experimental observables the CP effects are visible. From the discussion presented above we can see that they can be looked for in polarized angular distribution. And what about the unpolarized angular distribution? If CP is conserved then the helicity amplitude satisfies the relation (Θ and ϕ are CM scattering angles)

$$M(\sigma, \bar{\sigma}; \lambda_1, \lambda_2; \Theta, \phi) = -\eta_{CP}^*(1)\eta_{CP}^*(2) \times M(-\bar{\sigma}, -\sigma; -\lambda_1, -\lambda_2; \pi - \Theta, \pi + \phi). \quad (3.19)$$

If we sum over all helicity states the unpolarized angular distribution has

forward-backward isotropy

$$\frac{d\sigma}{d\Omega}(\Theta, \phi) = \frac{d\sigma}{d\Omega}(\pi - \Theta, \pi + \phi). \quad (3.20)$$

Does it mean that anisotropy can be observed if CP is violated? Unfortunately not, at least if we neglect the final state interaction. Without final state interaction from CPT symmetry we can prove the relation

$$M(\sigma, \bar{\sigma}; \lambda_1, \lambda_2; \Theta, \phi) = -\eta_{CP}(1)\eta_{CP}(2)e^{2i(\sigma-\bar{\sigma})(\pi+\phi)} \\ M^*(-\bar{\sigma}, -\sigma; -\lambda_1, -\lambda_2; \pi - \Theta, \pi + \phi) \quad (3.21)$$

from which the forward-backward isotropy also follows [53]. So the only observables where we can try to find the CP violation effect are the total cross sections and the polarized angular distributions. As the magnitudes of the total cross sections are larger in comparison with polarization angular distribution I will investigate now the total cross section $e^-e^+ \rightarrow N_1N_2$.

There are six phases which cause the CP symmetry breaking. I take the matrices m_D and M_R in the form

$$m_D = \begin{pmatrix} 1. & 1. & .9 \\ 1. & 1. & .9 \\ .9 & .9 & .95 \end{pmatrix}, \quad (3.22)$$

and

$$M_R = \begin{pmatrix} 150e^{i\alpha} & 10 & 20 \\ 10 & 200e^{i\beta} & 10 \\ 20 & 10 & 10^4e^{i\gamma} \end{pmatrix}, \quad (3.23)$$

which produce a reasonable spectrum of light neutrinos (see Section 2). If we compare these matrices with Eq.(3.18) we can see that if only one or more phases (α, β or γ) are not equal 0 or π the CP is violated. Two heavy neutrinos with masses $M_1 \simeq 150$ GeV and $M_2 \simeq 200$ GeV, almost independent of

the phases α, β and γ , result from this mass matrix. The appropriate mixing matrix elements $(K, K_R)_{1e}, (K, K_R)_{2e}$ depend on the phases α and β and are almost independent of the phase γ . For $\alpha = \beta = \gamma = 0$ two neutrinos have equal CP parity and CP is conserved for

$$\eta_{CP}(N_1) = \eta_{CP}(N_2) = +i. \quad (3.24)$$

For $\alpha = \pi, \beta = \gamma = 0$ CP is also conserved if we introduce the CP parities

$$-\eta_{CP}(N_1) = \eta_{CP}(N_2) = +i. \quad (3.25)$$

For any other values of phases CP is violated. The production cross sections versus energy are presented in Fig.4.

Two factors affect the behaviour of the cross section. Different α, β, γ in the matrix M_R cause that the mixing matrix elements $(K, K_R)_{eN_1}, (K, K_R)_{eN_2}$, which are a part of the unitary matrix U, change not only their phase factors but absolute values, too. So, firstly there is a real CP effect - phases in $(K, K_R)_{eN}$ matrix elements change with changing α, β, γ and cause different interferences among various diagrams. Secondly, different absolute values of mixing matrix elements are obtained that result also in changes of the cross section magnitude.

In Fig.4 both these effects are taken into account together. To find out the influence of CP phases only we fix in Fig.5 absolute values of mixing matrix elements to be constant with changing α, β, γ .

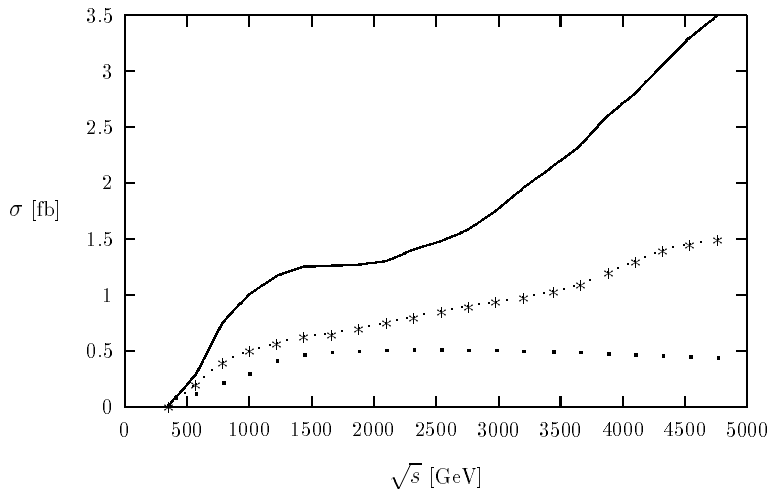


Fig.4. CP and mixing matrix effects for the $e^-e^+ \rightarrow N_1(150)N_2(200)$ production process. Solid line is for $\alpha = \beta = \gamma = 0$, dotted line is for $\alpha = \pi, \beta = \gamma = 0$ and the third line (with asterisks) is for $\alpha = 2.0, \beta = \gamma = 0$ phases.

We can see that the influence of the CP interference is very large. The cross section for production of two neutrinos with opposite CP parities can be several times larger than the cross section for production of the same CP parity neutrinos. The cross sections for the real CP breaking case are placed between two CP conserving situations.

We can see from Fig.4 and Fig.5 that the total cross section for production of two different heavy neutrinos equals a few femtobarns for $\sqrt{s} \leq 0(1)$ TeV. The cross section for production of two identical heavy neutrinos could be utmost ~ 30 times larger (compare $(K_R)_{1e}$ and $(K_R)_{2e}$ in Fig.5 caption). It could happen if the mixing angle $(K_R)_{Ne}$ have been maximal: $(K_R)_{Ne} \sim 1$. However, in this case CP effects disappear (see Eqs.(3.4)-(3.5)). These cross sections depend crucially on the mass of the additional gauge boson W_2 and

are negligible for the RHS model as a right-handed heavy neutrino couples very weakly to a gauge boson W^- .

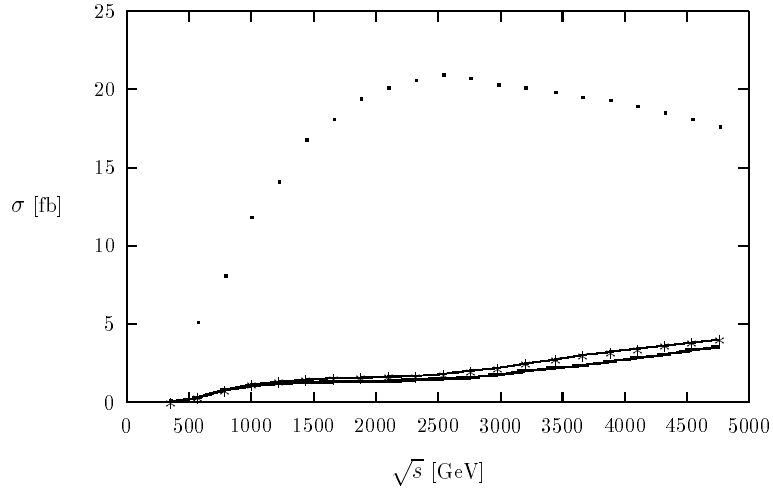


Fig.5. The pure CP violation effect caused by phases on the $e^-e^+ \rightarrow N_1(150)N_2(200)$ production process. Absolute values of mixing matrix elements for all lines are the same as the ones for the solid line in Fig.4. $[(K)_{1e} = 0.00535, (K_R)_{1e} = 0.9819, K_{2e} = 0.0058, (K_R)_{2e} = 0.189]$. The dotted (solid) line is for the opposite (the same) CP parity of neutrinos (Eqs.(3.25) and (3.24)); line with asterisks is for $\alpha = 2.0, \beta = \gamma = 0$, the same as in Fig.4.

All numerical results which have been shown till now in this Section have been connected with the ‘see-saw’ model. Because the mixing angles $(K_R)_{Ne}$ have been already of the order of 1 (e.g. maximal) we can expect that numerical results for two heavy neutrino production process are of the same order for the ‘non-decoupling’ model, too. Another situation will be, however, for a single heavy neutrino production process $e^-e^+ \rightarrow \nu N$ as a heavy neutrino-electron mixing angle K_{Ne} can be different for these models (Section 2). The situation for the ‘see-saw’ model is summarized in Fig.6 where the cross section as a heavy neutrino mass function is shown.

We can see that the values of the cross section are significant (range of few fb) only for small masses of a heavy neutrino. Now, in the last subsection I would like to focus on ‘non-decoupling’ effects in the single heavy neutrino production process.

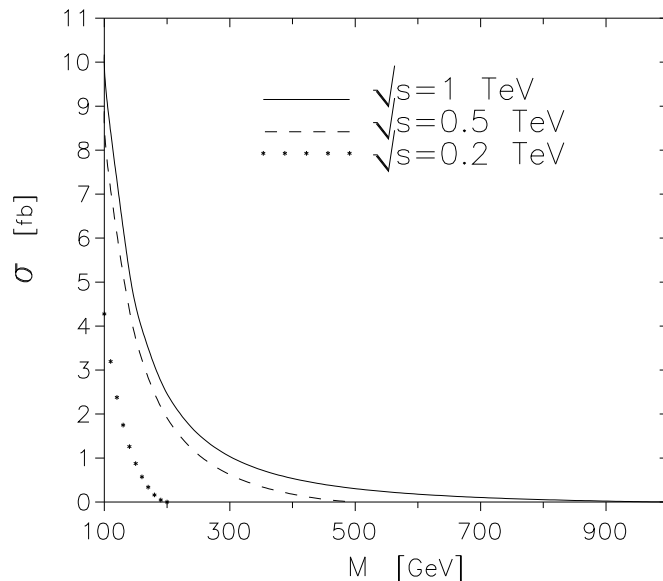


Fig.6. The cross section for the $e^-e^+ \rightarrow \nu N$ process in the framework of the classical ‘see-saw’ models. Solid, dashed lines and the line with stars are for 1 TeV, 500 GeV and 200 GeV CM energies of future colliders, respectively.

3.3 ‘Non-decoupling’ model and a heavy neutrino in the e^-e^+ collision

As it has been already shown in Section 2 the maximal mixing angle K_{Ne} depends on the number of neutrinos.

- $n_R = 1$ (or all heavy neutrinos with the same η_{CP} ’s)

According to Eq.(2.23) mixing angle K_{Ne} depend crucially on ω . Results for this case are given in Table 3.

M_N [GeV]	σ_{max}^{total} [fb], $n_R = 1$		
	$\sqrt{s} = 0.5$ TeV	$\sqrt{s} = 1$ TeV	$\sqrt{s} = 2$ TeV
100	0.18	0.2	0.2
150	0.25	0.3	0.3
200	0.31	0.4	0.4
300	0.34	0.6	0.6
500	-	0.8	1.0
700	-	0.7	1.3
1000	-	-	1.6

Table 3: The total cross section $\sigma_{tot}(e^+e^- \rightarrow \nu N)$ in $n_R = 1$ case (see Eq.(2.23) with $\omega^2 = 2 \cdot 10^{-5} TeV^{-1}$) for various heavy neutrino masses and three different total energies $\sqrt{s} = 0.5, 1, 2$ TeV.

As the maximal value of the K_{Ne} parameter is proportional to M_N the cross section is an increasing function of a heavy neutrino mass with exception at the end of the phase space $M_N \rightarrow \sqrt{s}$. Results are miserable⁷.

⁷The last results obtained for ω [42] can increase these values by a factor ~ 40 and then $n_R = 1$ case can focus some interest, too.

- $n_R = 2$

Taking into account Eqs.(2.28-2.29) in Fig.7 the cross section for $e^+e^- \rightarrow N\nu$ process as a function of the lighter neutrino's mass for different values of $A = \frac{M_2}{M_1}$ factor and for $\sqrt{s} = 1$ TeV is depicted. There is space for large σ but only for very small mass differences ($M_1 \simeq M_2$) - see Eq.(2.31). I take maximal κ^2 that equals to 0.0054 (Eq.(2.16)).

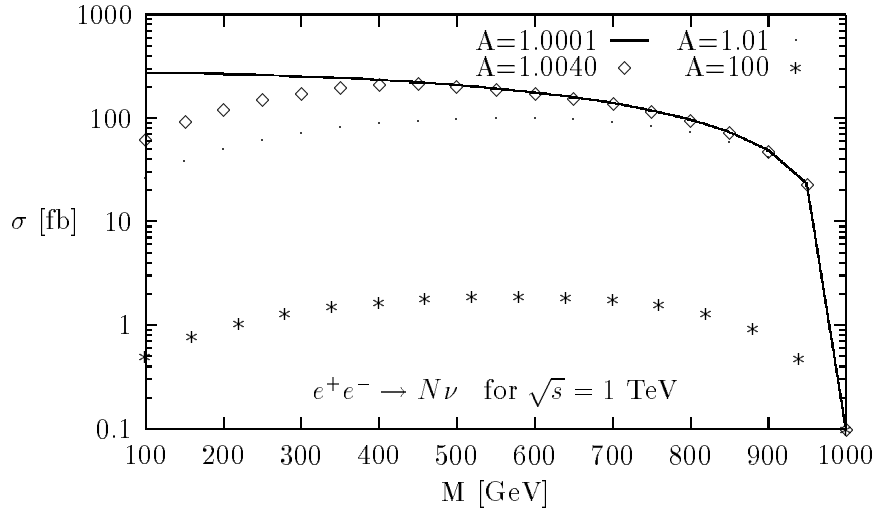


Fig.7. The cross section for the $e^+e^- \rightarrow N\nu$ process as a function of a heavy neutrino mass $M_1 = M$ for $\sqrt{s} = 1$ TeV in the models with two heavy neutrinos ($n_R = 2$) for different values of $A = \frac{M_2}{M_1}$ (solid line with $A = 1.0001$, ' \diamond ' line with $A = 1.004$, dots line with $A=1.01$ and ' $*$ ' line with $A=100$). Only for a very small mass difference $A \sim 1$ the existing experimental data leave the chance that the cross section is large, e.g. $\sigma_{max}(M = 100 \text{ GeV}) = 275 \text{ fb}$. If $M_2 \gg M_1$ then the cross section must be small, e.g. for $A = 100$, $\sigma_{max}(M = 100 \text{ GeV}) \simeq 0.5 \text{ fb}$.

- $n_R = 3$

Results for this case are gathered in Fig.8. We have three heavy neutrinos with masses $M_1 = M, M_2 = AM, M_3 = BM$ and $\eta_{CP}(N_1) = \eta_{CP}(N_2) =$

$-\eta_{CP}(N_3) = +i$ (see Section 2). Then the maximal mixing angle of the lightest heavy neutrino is ($A \rightarrow \infty, B \rightarrow 1$) $K_{N_1e}^2 = \frac{\kappa^2}{2}$ (Eq.(2.36)). The lower of two lines for each of CM energies depicted in Fig.8 realizes this case. The upper line is for the third of heavy neutrinos when its mixing angle is maximal, too. It can happen when $B = \frac{M_3}{M_1}$ is as big as possible (Eq.(2.36)), so I take $M_1 = 100$ GeV and parameterize the mixing angle of the third heavy neutrino as follows

$$(K_{N_3e})^2 = \frac{\left(\frac{M}{100 \text{ GeV}}\right) \kappa^2}{1 + \left(\frac{M}{100 \text{ GeV}}\right)}. \quad (3.26)$$

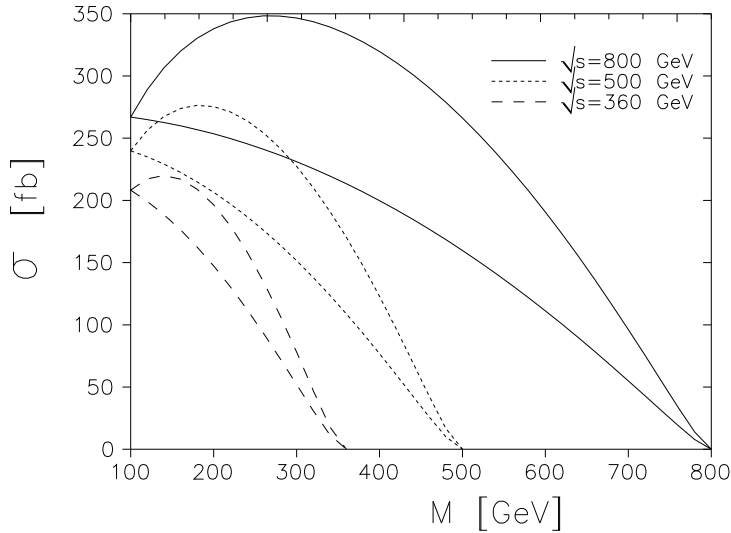


Fig.8 Production of a single heavy neutrino ($e^-e^+ \rightarrow \nu N$) with maximal possible mixing angle K_{Ne} for different CM energies: $\sqrt{s} = 360, 500, 800$ GeV as a function of heavy neutrino mass. The lower line in each pair is for the lightest of heavy neutrinos, the upper is for the third of heavy neutrinos with mass M and the mixing angle given by Eq.(3.26).

As it was already mentioned the results for the LR and the RHS models are practically the same for the single heavy neutrino production (see Table

1). That is why the results given in Fig.8 can be assumed to describe these two models altogether. We can see that the results for the ‘non-decoupling’ model are more optimistic than for the ‘see-saw’ one and it is worth to study what we can find in reality in a collision [54]. Heavy neutrinos which I consider are unstable. Possible decay channels are $N \rightarrow W^\pm l^\mp$, $N \rightarrow Z \nu_l$ and $N \rightarrow H \nu_l$. Two first are always opened for $M_N \geq 100$ GeV, the last one depends on Higgs particle’s mass.

The total decay width equals to

$$\Gamma_N = \sum_l \left(2\Gamma(N \rightarrow l^+ W^-) + \Gamma(N \rightarrow \nu_l Z) + \Gamma(N \rightarrow \nu_l H) \Theta(m_N - m_H) \right) \quad (3.27)$$

where

$$\begin{aligned} \sum_l \Gamma(N \rightarrow l^+ W^-) &\propto \sum_{l=e,\mu,\tau} |K_{Nl}|^2 \simeq |K_{Ne}|^2, \quad (3.28) \\ \sum_l \Gamma(N \rightarrow \nu_l H), \sum_l \Gamma(N \rightarrow \nu_l Z) &\propto \sum_l |\Omega_{N\nu_l}|^2 \simeq \sum_l |K_{Nl}|^2 \simeq |K_{Ne}|^2. \end{aligned} \quad (3.29)$$

In the approximations made in Eqs.(3.28) and (3.29) it is assumed that in each column of K matrix ($l = e, \mu, \tau$)

$$(K_{\nu_e l}, K_{\nu_\mu l}, K_{\nu_\tau l}, K_{N_1 l}, K_{N_2 l}, \dots)^T$$

only one coupling between heavy neutrinos and lepton is visible $K_{N_i l} \simeq K_{Ne}$. All other couplings are very small and are neglected.

If we also assume lepton universality ($K_{\nu_l l} \simeq 1$) then also the production cross section can be parameterized by only one mixing angle

$$\sigma_{tot} = \sum_{i=e,\mu,\tau} \sigma(e^+ e^- \rightarrow \nu_i N), \quad (3.30)$$

and

$$\sigma_{tot} \propto |K_{Ne}|^2 \left(|K_{\nu_e e}|^2 + |K_{\nu_\mu}|^2 + |K_{\nu_\tau}|^2 \right)$$

$$= |K_{Ne}|^2 \left(1 - \sum_N |K_{Ne}|^2\right)^2 \simeq |K_{Ne}|^2. \quad (3.31)$$

In this way we have only one parameter K_{Ne} which is important in the neutrino production-decay process.

So, let's discuss the angular distribution for the final electron (positron) in the process

$$e^+e^- \rightarrow \nu N \quad (3.32)$$

$$\hookrightarrow e^\pm W^\mp$$

where for N I take the lightest of heavy neutrinos.

Numerical results are gathered on the next three Figures.

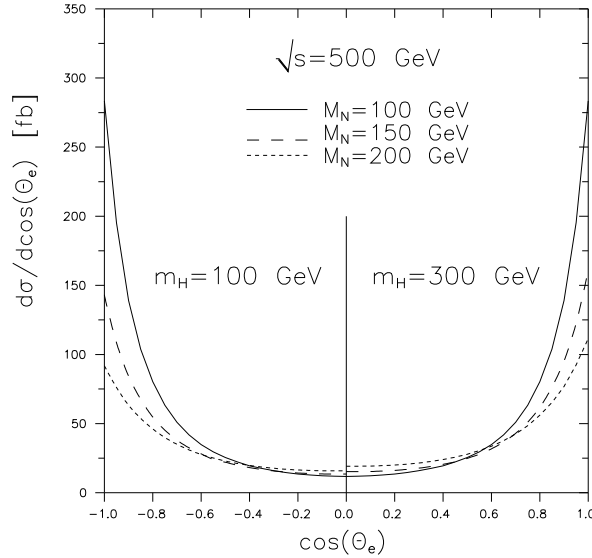


Fig.9. Distribution of the final electron from a heavy neutrino decay for $\sqrt{s} = 500$ GeV collider with $M_N = 100$ GeV (solid line), $M_N = 150$ GeV (long-dashed line) and $M_N = 200$ GeV (short-dashed line). Left half of the Figure gives results for $m_H = 100$ GeV, right half of the Figure for $m_H = 300$ GeV (Higgs decay channel is closed).

In Fig.9 I present the angular distribution for the final electron $e^-e^+ \rightarrow \nu(N \rightarrow e^-W^+)$ for various masses of heavy neutrino $M_N = 100, 150$ and 200 GeV calculated for the maximal possible $|K_{Ne}|^2 \simeq \frac{\kappa^2}{2}$ ($\kappa^2 = 0.0054$). Results

are given for the NLC with $\sqrt{s} = 500$ GeV. This distribution has forward-backward symmetry. To show the influence of Higgs particle I include results for $m_H = 100$ GeV on the left half of the Figure ($-1 \leq \cos \Theta_e \leq 0$) and on the right side ($0 \leq \cos \Theta_e \leq 1$) for $m_H = 300$ GeV. For a higher Higgs mass the total width Γ_N is smaller due to the greater value of the branching ratio for the $N \rightarrow lW$ decay and the cross section $\frac{d\sigma}{d\cos\Theta_e}$ is larger. Numerically, Higgs has no influence on the cross section for $M_N = 100$ GeV (for $m_H = 100 \div 300$ GeV $N \rightarrow \nu H$ decay channel is closed) and the influence of the Higgs particle is approximately equal to 10 %, 15% for $M_N = 150, 200$ GeV, respectively (only the decay mode with $m_H = 100$ GeV is opened in this case).

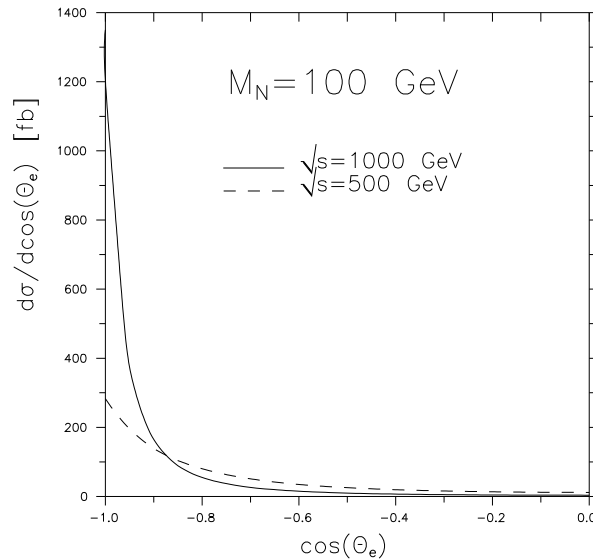


Fig.10 Backward distribution of the final electron coming from a heavy neutrino decay ($M_N = 100$ GeV) for two different energies: $\sqrt{s} = 500$ GeV (dashed line) and $\sqrt{s} = 1000$ GeV (solid line).

For higher energies the final electron distribution is more peaked in the forward-backward direction ($\cos \Theta_e = \pm 1$). This is the result of W^\pm exchange in t and u channels. As an example I have compared the final electron

distribution from the decay of a heavy neutrino with mass $M_N = 100$ GeV for $\sqrt{s} = 500$ GeV and $\sqrt{s} = 1000$ GeV energies (Fig.10).

Finally in Fig.11 I present the angular distribution $\frac{d\sigma}{d\cos\Theta_e}$ for various masses of heavy neutrino $M_N = 100, 300$ and 500 GeV ($m_H = 100$ GeV). The cross section becomes higher and more peaked in the forward-backward direction for a smaller mass of heavy neutrinos. The effect of growing $\frac{d\sigma}{d\cos\Theta_e}$ is the result of increasing $BR(N \rightarrow lW)$ and increasing $\sigma_{tot}(e^+e^- \rightarrow \nu N)$ for smaller M_N . The effect of slope reduction with M_N mass in the forward-backward direction is also kinematically understandable.

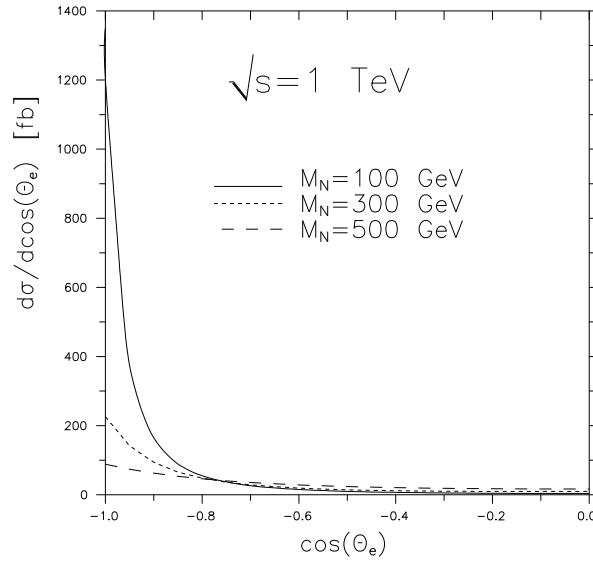


Fig.11. Backward distribution of the final electron coming from a heavy neutrino decay with mass $M_N = 100$ GeV (solid line), $M_N = 300$ GeV (short-dashed line) and $M_N = 500$ GeV (long-dashed line) for $\sqrt{s} = 1$ TeV.

Backward distribution of the electron coming from a heavy neutrino decay gives a chance for a heavy neutrino detection. The main background for this process is the production of W^+W^- pair with the decay $W^- \rightarrow e^-\nu$. The distribution of the electron coming from the heavy neutrino decay (N)

and from W 's decay by $e^+e^- \rightarrow W^+W^-$ process differs very much in the forward-backward direction. For a high energy ($\sqrt{s} > 0.5$ TeV) the angular distribution of electrons coming from the W^- decay is peaked in the forward direction. On the contrary, the e^- coming from the N decay will travel equally well both in forward and backward direction.

4 Indirect heavy neutrinos detection in e^-e^- collision: $e^-e^- \rightarrow W^-W^-$ process

The $e^-e^- \rightarrow W^-W^-$ process was firstly proposed in 1982 ([55], see also [56]) as one of tests for the lepton number violation. As it can be seen from Fig.12 this process is sensible to all neutrinos, light and heavy. In the RHS model only t and u channels are present while in the LR model doubly charged Higgs particles are important, too. They introduce resonances and are needed for proper high-energy behaviour of the cross section [55],[57].

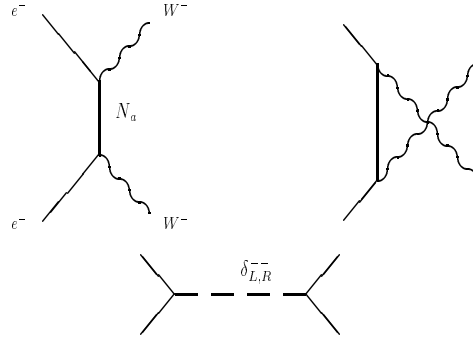


Fig.12. The tree level Feynman diagrams which contribute to the $e^-e^- \rightarrow W^-W^-$ process. In the LR model all three channels are present, while in the RHS model s-channel is absent.

I give up here a detailed analysis of the additional processes that can appear in the LR model ($e^-e^- \rightarrow W_1^-W_2^-$, $e^-e^- \rightarrow W_2^-W_2^-$) and I will focus on SM gauge bosons production. Because of kinematical reasons these additional processes can be of special importance not before a collider with $\sqrt{s} \simeq 1$ TeV energy will appear. For such energies, especially when W_2^- would be not too heavy (let's say $M_{W_2} \simeq 600$ GeV that is close to the present experimental limit [21],[22]) the W_2^- would be easily discovered unless the

energy of collider would be too close to the threshold [57],[58].

Without heavy neutrinos the process $e^-e^- \rightarrow W^-W^-$ is negligible small. The reason is that light (left-handed) neutrinos are (almost) massless and such conditions cause that Majorana neutrinos are not distinguishable from Dirac neutrinos (actually they decouple to Weyl spinors) [59] and the lepton number is conserved (see [23] for details). Contribution of a left-handed doubly charged Higgs particle in s-channel is negligible, too [60]. Apart from heavy neutrinos, δ_R^{--} right-handed resonance is important for this process, too. This case will be discussed later.

I give up here writing down the helicity amplitudes for this process. They can be found in [43],[57]. Two facts are important. Firstly, as all heavy neutrinos are exchanged, the amplitude is a sum of all of them. Secondly, we have checked that for the $e^-e^- \rightarrow W^-W^-$ process the helicity amplitudes with purely left-handed or purely right-handed electrons, proportional to the heavy neutrino masses, are dominant [57]. These helicity amplitudes include either a square of the K mixing matrix elements ($e_L^-e_L^-$ collision) or a square of the K_R ones ($e_R^-e_R^-$ collision). That is why these two facts cause that interferences among contributions from different neutrinos can appear if some K or K_R elements are complex. Let's discuss these effects more carefully now.

4.1 CP violation effects in the $e^-e^- \rightarrow W^-W^-$ process ('see-saw' model)

Similarly to the discussion of CP effects in the $e^-e^+ \rightarrow \nu N$ process (Section 3) we choose the neutrino mass matrix M_R in the form

$$M_R = \begin{pmatrix} e^{i\alpha}M & 10 & 20 \\ 10 & 2e^{i\beta}M & 10 \\ 20 & 10 & 3e^{i\gamma}M \end{pmatrix}. \quad (4.1)$$

Matrix m_D is the same as in Eq.(3.22).

Fig.13 gives results for the LR model where the above parameterization was used.

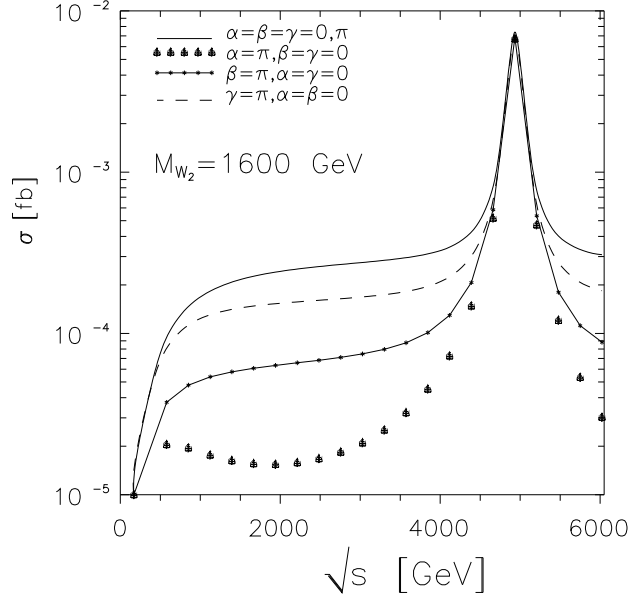


Fig.13. Process $e^-e^- \rightarrow W_1^-W_1^-$ (LR model) for $M_1 = 200$ GeV, $M_2 = 400$ GeV, $M_3 = 600$ GeV (Eq.(4.1)) and $M_{W_2} = 1600$ GeV when CP parity is conserved in the lepton sector.

The shape of these lines can be understood in the following way.

If all diagonal elements M_i ($i=1,2,3$) of the matrix M_R (Eq.(4.1)) are real and positive ($\alpha = \beta = \gamma = 0$) then the eigenvalues of the neutrino mass matrix are also positive and the CP symmetry is conserved if the CP parities of heavy neutrinos are the same and equal

$$\eta_{CP}(N_4) = \eta_{CP}(N_5) = \eta_{CP}(N_6) = +i. \quad (4.2)$$

The same happens when all masses M_1, M_2, M_3 are real, negative ($\alpha = \beta = \gamma = \pi$). Then CP is also conserved if CP parities of neutrinos are negative,

imaginary

$$\eta_{CP}(N_4) = \eta_{CP}(N_5) = \eta_{CP}(N_6) = -i. \quad (4.3)$$

In both cases above the mixing matrix elements $(K, K_R)_{ei}$, $i=4,5,6$ are either pure real ($\alpha = \beta = \gamma = 0$) or pure imaginary ($\alpha = \beta = \gamma = \pi$). As it was already mentioned the dominant helicity amplitudes include either a square of the K mixing matrix elements ($e_L^- e_L^-$ collision) or a square of the K_R ones ($e_R^- e_R^-$ collision) and a summation must be carried out over all exchanged heavy neutrinos. That is why constructive contribution from all heavy neutrinos is present for $\alpha = \beta = \gamma = 0, \pi$ (solid line on Fig.13). In the case of mixing CP parities the CP symmetry is also conserved but the destructive interference between contributions from various neutrinos causes that the cross section decreases. In this case some of $(K, K_R)_{ei}$, $i=4,5,6$ matrix elements are real and some are imaginary.

To obtain these CP effects several K or K_R matrix elements must interfere in the same helicity amplitude. The structure of the chosen neutrino mass matrix causes that K_{en} $n=4,5,6$ matrix elements are of the similar order

$$|K_{e4}| \simeq \frac{1}{M_4} > |K_{e5}| \simeq \frac{1}{M_5} > |K_{e6}| \simeq \frac{1}{M_6} \quad (4.4)$$

but only one suitable element of the K_R matrix is large (see Eq.(2.11))

$$|K_R|_{e4} \sim 1 \gg |(K_R)_{ei}| \quad i = 5, 6. \quad (4.5)$$

This property causes that only if the K matrix elements contribute to the cross section in the visible way ($e_L^- e_L^-$ collision), the CP breaking is seen. It is just the case for two light gauge bosons $W_1^- W_1^-$ production where W_1^- couples predominantly with left-handed electrons (Eq.(B.21)). If the contribution with $e_R^- e_R^-$ helicity amplitude becomes important, then the CP symmetry effect decreases. That is why the effect is visible only outside the

δ_R^{--} resonance region where only one right-handed mixing matrix K_R gives essential contribution (Eq.(4.5)) and the interference has no importance. It also means that the CP symmetry effect is more visible for the larger M_{W_2} , when $\cos \xi \rightarrow 1$ (Eq.(B.21)).

If the CP symmetry is violated (phases $\alpha, \beta, \gamma \neq 0, \pi$), the cross sections lie between two limiting lines in Fig.13.

The effects of the CP symmetry in the RHS model is depicted in Fig.14. For the same energy with the same mass matrix parameterization the effects are practically the same as those in the L-R model.

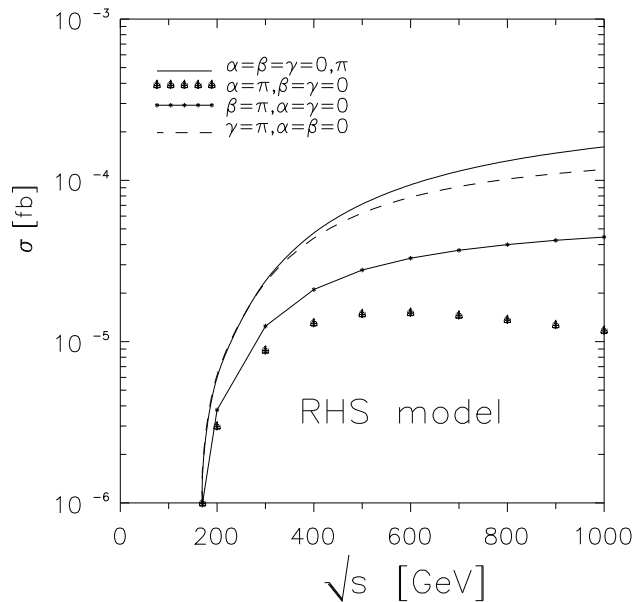


Fig.14. Process $e^-e^- \rightarrow W_1^-W_1^-$ (RHS model) for $M_1 = 200$ GeV, $M_2 = 400$ GeV, $M_3 = 600$ GeV when CP parity is conserved in the lepton sector.

We can see that although CP effects are quite interesting the cross sections are very small. It is shown in Fig.15 where the cross section as the function of heavy neutrino mass is carried out for a classical ‘see-saw’ model ($K_{Ne} \sim 1/M_N$).

The signal from the $e^-e^- \rightarrow W^-W^-$ process is so clean (the only impor-

tant SM background comes from the $e^-e^- \rightarrow W^-W^- \nu_e \nu_e$ process [61] and can be suppressed by appropriate kinematical cuts) that as small as $\sigma = 0.1$ fb cross section is enough for possible process discovery [62].

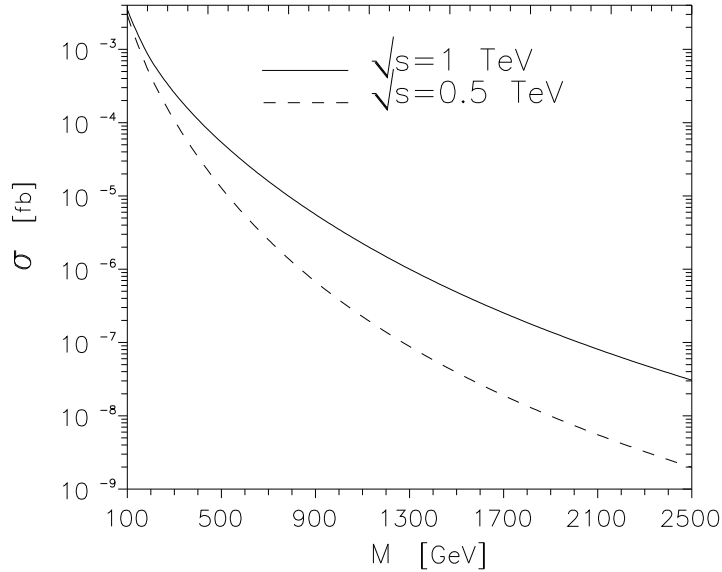


Fig.15. The cross section for the $e^-e^- \rightarrow W^-W^-$ process as a function of the heavy neutrino mass for the classical ‘see-saw’ models, where the mixing angles between light and heavy neutrinos are proportional to the inverse of mass of the heavy neutrino.

However, as we know from previous sections we can expect that results can be quite different for ‘non-decoupling’ models.

4.2 ‘Non-decoupling model and the $e^-e^- \rightarrow W^-W^-$ process

Now I would like to establish how big the utmost cross section for the $e^-e^- \rightarrow W^-W^-$ process can be. We can find in literature quite optimistic estimations for that [63]. I will show here similarly to the $e^-e^+ \rightarrow \nu N$ case how ‘maximal’ results depend on the number of heavy neutrinos.

- $n_R = 1$

If CP parities of all heavy neutrinos are the same or we have only one right-handed neutrino then the $e^-e^- \rightarrow W^-W^-$ process is very small, much below $\sigma = 0.1$ fb (here a very restrictive bound on mixing angle K_{Ne} (Eq.(2.23)) and the proportionality of the cross section to the fourth power of this factor are crucial).

- $n_R = 2$

We can have here large K_{Ne} values (Eq.(2.31)) but only when $A \rightarrow 1$ so two degenerate Majorana neutrinos ($M_1 = M_2$) with opposite CP parities appear which correspond to a one Dirac neutrino. As a Dirac neutrino conserves the lepton number the cross section vanishes. It can be understood easily in a different way, too. Helicity amplitudes are proportional to K_{Ne}^2 mixing (two the same vertices in t and u channels (Fig.12)) and the amplitude is a sum over two exchanged heavy neutrinos of equal mass. Then contributions from these two neutrinos are the same apart from a relative sign which is opposite (K_{Ne} 's are pure real and complex for them).

- $n_R = 3$

The case with $n_R = 3$ changes situation and the most optimistic results for this case are shown in Fig.16. Taking $\eta_{CP}(N_1) = \eta_{CP}(N_2) = -\eta_{CP}(N_3) = i$ and $M_1 = M$, $M_2 = AM$, $M_3 = BM$ we can find values A,B (masses of heavy neutrinos) for which mixings of heavy neutrinos are such (Eqs.(2.32)-(2.35)) that $\sigma(e^-e^- \rightarrow W^-W^-)$ reaches the maximal value⁸. This situation

⁸Careful reader could noted contradiction between conclusions about CP effects in previous subsection ('see-saw' model) and this given for the 'non-decoupling' model. In Figs.13,14 the solid line represents constructive interferences among different heavy

takes place for a very heavy second ($A \gg 1$) and a heavier third neutrino ($B \sim 2 - 10$). In this Figure I depict also the cross section for production of the lightest heavy neutrinos with the mass M in the $e^+e^- \rightarrow \nu N$ process taking exactly the same mixing angle K_{N_1e} as for the $e^-e^- \rightarrow W^-W^-$ process.

We can see that

(i) everywhere in the possible region of phase space the production of heavy neutrinos in the e^+e^- process has greater cross section than the lepton violating process e^-e^- . It is impossible to find such mixing angles and masses which would show the opposite.

(ii) there are regions of heavy neutrino masses outside the phase space for their production in the e^+e^- process where the $\Delta L = 2$ process $e^-e^- \rightarrow W^-W^-$ is still a possible place to look for heavy neutrinos. It is a small region $1 \text{ TeV} < M < 1.1 \text{ TeV}$ for $\sqrt{s} = 1 \text{ TeV}$, $1.5 \text{ TeV} < M < 2 \text{ TeV}$ for $\sqrt{s} = 1.5 \text{ TeV}$ and $2 \text{ TeV} < M < 3.1 \text{ TeV}$ for $\sqrt{s} = 2 \text{ TeV}$ where the cross section $\sigma(e^-e^- \rightarrow W^-W^-)$ is still above the ‘detection limit’. There is no such place with the $\sqrt{s} = 0.5 \text{ TeV}$ collider. The experimental value of κ^2 (see Eq.(2.16)) would have to be below $\sim 0.004, \sim 0.003, \sim 0.002$ for $\sqrt{s} = 1, 1.5, 2 \text{ TeV}$ respectively to cause these regions to vanish.

neutrinos contributions - cross section is the biggest (CP parities of heavy neutrinos are the same). For the ‘non-decoupling’ model, however, biggest results can be obtained when neutrinos have unlike CP parities (Section 2). The reason for this is that for the ‘non-decoupling’ model contribution of some heavy neutrino with mixing angle K_{Ne} dominates over others and CP effects as discussed for the ‘see-saw’ model vanish (K_{Ne} ’s in the ‘see-saw’ model are comparable and interferences can appear (Eq.(4.4)). As $(K_{Ne})_{non-dec.} \gg (K_{Ne})_{see-saw}$ and consequently $\sigma(e^-e^- \rightarrow W^-W^-)_{non-dec.} \gg \sigma(e^-e^- \rightarrow W^-W^-)_{see-saw}$ the conclusions about CP effects are quite different.

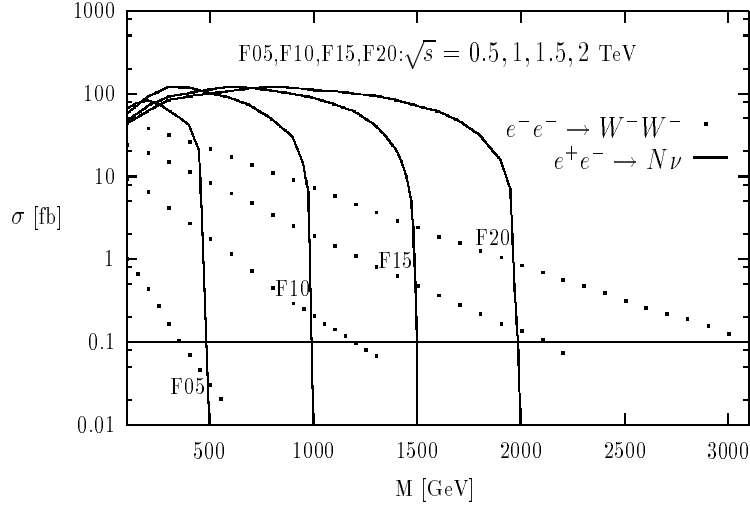


Fig.16. The cross sections for the $e^+e^- \rightarrow N\nu$ and $e^-e^- \rightarrow W^-W^-$ processes as a function of the lightest neutrino mass $M_1 = M$ for different CM energies (the curves denoted by F05, F10, F15 and F20 depicted the cross section for both processes for $\sqrt{s}=0.5, 1, 1.5$ and 2 TeV respectively) for $n_R = 3$. The cross sections for the $e^-e^- \rightarrow W^-W^-$ process are chosen to be the largest. For the $e^+e^- \rightarrow N\nu$ reaction the cross section for each of neutrino masses is calculated using the same parameters as for $\sigma(e^-e^- \rightarrow W^-W^-)$. The solid line parallel to the M axis gives the predicted ‘detection limit’ ($\sigma = 0.1$ fb) for the $e^-e^- \rightarrow W^-W^-$ process.

The above results are exact for the RHS model. In the LR model the situation is different as doubly charged Higgs particles exist and a resonance can appear. This situation is summarized on Fig.17 [60].

The total decay width for the δ_R^- is taken to be 10 GeV. We can see that even for CM energies $\sim 4\Gamma_{\delta_R^-}$ out of resonance peak the s channel contribution dominates over t and u channel ones. The reason is that for $\sqrt{s} \leq 500$ GeV contributions of t and u channels are below $\sigma = 0.1$ fb for almost all allowed space of parameters (see Fig.16). Specially promising results are when M_{W_2} is very close to its experimental limit ([21]).

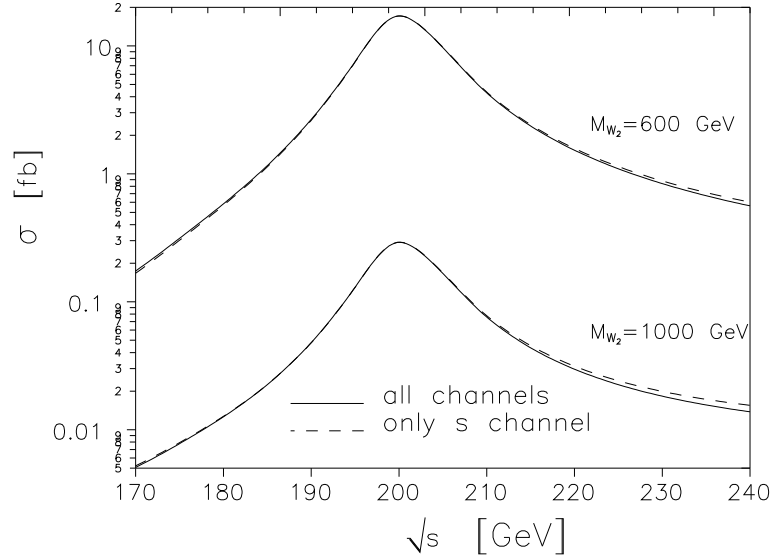


Fig.17. The cross sections for the $e^-e^- \rightarrow W^-W^-$ process with δ_R^{--} resonance ($M_{\delta_R^{--}}=200$ GeV) as a CM energy function. The solid line represents the total cross section with contribution from t,u and s channels altogether, the dashed line depicts the cross section after removing contributions of t and u channels.

We would like to point out that doubly charged Higgs particle detection in s channel would also indicate that heavy neutrinos exist. The reason is that coupling of the δ_R^{--} Higgs particle with electrons is proportional to neutrino masses and the light neutrinos alone are not sufficient to give detectable s-channel signal in the $e^-e^- \rightarrow W^-W^-$ process [60].

5 Conclusions

None of the nonstandard processes involving a heavy neutrino has ever been detected. In this Thesis I have discussed possibilities of their detection by the $e^-e^+ \rightarrow \nu N$ and the $e^-e^- \rightarrow W^-W^-$ processes which are the most promising reactions in the NLC. Cross sections for these processes are very sensitive to the heavy neutrino mixing angle with an electron ($\sigma(e^-e^+ \rightarrow \nu N) \sim K_{Ne}^2$, $\sigma(e^-e^- \rightarrow W^-W^-) \sim K_{Ne}^4$). In the framework of the ‘see-saw’ class of models this mixing angle is connected with a heavy neutrino mass and because this mass is large ($> M_Z$) the mixing angle is small and decreases with a heavy neutrino mass. It causes that cross sections are very small for the $e^-e^+ \rightarrow \nu N$ process and detectable only for not too heavy neutrinos (Fig.6). CP effects are important when two heavy neutrinos are produced (no helicity suppression factors above threshold) with the changes in the cross sections which result from the CP breaking phases and which can be several times larger than the cross sections themselves (Figs.4 and 5). Although CP effects are quite interesting in the framework of the ‘see-saw’ model for the $e^-e^- \rightarrow W^-W^-$ process, too (Figs.13,14), the values of cross sections are so small that there is practically no chance for process detection (Fig.15). However, there are other (‘non-decoupling’) models where mixing angles are independent of heavy neutrino masses and can be large - the only restriction on their values comes from experimental data. The goal of this Thesis has been to show that taking into account all stringent limits on heavy neutrino mixing angles and masses the heavy neutrinos can still be detected through both the $e^-e^+ \rightarrow \nu N$ process (Figs.7-11) and the $e^-e^- \rightarrow W^-W^-$ process (Figs.16-17) in future linear colliders. From the results given there we can also deduce how much those low-energy limits would have to change

in future to cause that these processes would be below detection and also, what possibly detection would tell us about heavy neutrinos themselves. It appears that to get significant cross sections the two characteristics of heavy neutrinos are crucial: their number and CP eigenvalues. The detectable cross sections can be obtained only when $n_R > 1$ and when heavy neutrinos have unlike CP parities. Then the cross section for the $e^-e^+ \rightarrow \nu N$ process can be as large as $\sigma \simeq 275$ fb for $n_R = 2$ and $\sqrt{s} = 1$ TeV (and similarly for $n_R > 2$) and heavy neutrinos can be discovered by electrons detection in the $e^-e^+ \rightarrow \nu(N \rightarrow e^-W^+)$ chain (backward distribution).

The cross section for the $e^-e^- \rightarrow W^-W^-$ process is still under detection when $n_R = 2$. If $n_R = 3$ then there is a possible space of heavy neutrino-electron mixing angles and heavy neutrino masses where the process $e^-e^- \rightarrow W^-W^-$ can be detected for $\sqrt{s} \geq 500$ GeV. For $\sqrt{s} \leq 500$ GeV the δ_{R^-} resonance (LR model) can enhance the process ($e_R^-e_R^-$ collision) specially when a mass of the additional charged gauge boson is below 1 TeV. The discovery of the doubly charged Higgs particle through the e^-e^- s-channel resonance would be also an (indirect) indication that heavy neutrinos exist.

6 Appendix A. Neutrino mass matrices, their diagonalization and mixing matrices

I consider two types of gauge models.

RHS model

This model is based on $SU(2)_L \otimes U(1)_Y$ gauge group. The left handed lepton fields are put in doublets and transformed according to $SU(2)$ representation (the quantum numbers of weak isospin and hypercharge (T_{3L}, Y) are given in brackets)

$$L_{iL} = \begin{pmatrix} \nu_{l_j} \\ l_j^- \end{pmatrix}_L \quad : \begin{matrix} (1/2, -1) \\ (-1/2, -1) \end{matrix}, \quad l_j = e, \mu, \tau, \quad (\text{A.1})$$

meanwhile the right-handed lepton fields are $SU(2)$ singlets

$$\begin{aligned} l_{jR} = e_R^-, \nu_R^-, \tau_R^- & \quad : (0, -2), \\ \nu_{jR} = \nu_{1R}, \nu_{2R}, \dots & \quad : (0, 0). \end{aligned} \quad (\text{A.2})$$

The only difference between this model and the standard, GWS model is caused by the presence of the right-handed neutrino fields. The remaining part of the model is exactly the same (quark, Higgs sector). That means that the lepton part of the Lagrangian allowed by the gauge symmetry is the following

$$\begin{aligned} L_{leptons} = i\bar{L}_L D L_L + i\bar{l}_R D l_R + i\bar{\nu}_R D \nu_R \\ - h^l [\bar{L}_L \tilde{\phi} l_R] - h^\nu [\bar{L}_L \phi \nu_R] - \frac{1}{2} \bar{\nu}_L^c (M_R) \nu_R + h.c. \end{aligned} \quad (\text{A.3})$$

where ϕ denotes a Higgs doublet ($\tilde{\phi} = \epsilon \phi^* = (\phi^+, -\phi^{0*})^T$)

$$\phi = \begin{pmatrix} \phi^0 \\ \phi^- \end{pmatrix} = \frac{1}{\sqrt{2}} \begin{pmatrix} v + H^0 + i\chi^0 \\ \chi^- \end{pmatrix}, \quad (\text{A.4})$$

$D = \gamma^\mu D_\mu$ and covariant derivative has the form

$$D_\mu = \begin{cases} \partial_\mu - ig\frac{\vec{\tau}}{2}\vec{W}_\mu - \frac{ig'}{2}YB_\mu & \text{for doublets} \\ \partial_\mu - \frac{ig'}{2}YB_\mu & \text{for singlets.} \end{cases} \quad (\text{A.5})$$

Matrices h^l, h^ν of 3×3 and $3 \times (3 + n_R)$ dimensions, respectively, describe couplings of lepton fields with Higgs fields and the symbol ‘ v ’ in Eq.(A.4) describes Standard Model’s vacuum expectation value. So, besides lepton-Higgs field couplings the Lagrangian include mass terms for leptons

$$L_{mass} = -\bar{l}_L m^l l_R - \bar{\nu}_L m_D \nu_R - \frac{1}{2} \bar{\nu}_L^c (M_R) \nu_R + h.c. \quad (\text{A.6})$$

$$m_D = \frac{h^\nu v}{\sqrt{2}}, \quad m^l = \frac{h^l v}{\sqrt{2}}. \quad (\text{A.7})$$

Full mass Lagrangian for neutrinos can be rewritten as follows

$$L_{mass}^{neutrinos} = -\frac{1}{2} (\bar{\nu}_L, \bar{\nu}_L^c) \begin{pmatrix} 0 & m_D \\ m_D^T & M_R \end{pmatrix} \begin{pmatrix} \nu_R^c \\ \nu_R \end{pmatrix} + h.c. \quad (\text{A.8})$$

where neutrino mass matrix M_ν has $(3 + n_R) \times (3 + n_R)$ dimension

$$M_\nu = \begin{pmatrix} \overbrace{0}^3 & \overbrace{\widehat{m}_D}^{n_R} \\ \overbrace{m_D^T}^3 & \overbrace{M_R}^{n_R} \end{pmatrix} \begin{matrix} \}3 \\ \}n_R \end{matrix}. \quad (\text{A.9})$$

Perturbative calculations demand to have $|h^\nu|_{ij}, |h^l|_{ij} \leq 1$, so all elements of the m_D matrix (3×3 dimension) are utmost of the order of charged lepton masses. Then, if we want to be consistent with the experimental data, matrix M_R of the $n_R \times n_R$ dimension must fullfil inequalities $(m_D)_{ij} \ll (M_R)_{ij} \geq 100$ GeV.

We can construct Majorana neutrinos ($\nu_M = \nu_M^C$)

$$\nu_M = \nu_R + \nu_L^c \quad (\text{A.10})$$

and then, using unitary matrix U in the form

$$U = \left(\begin{array}{c} \overbrace{U_L^*}^{3+n_R} \\ U_R \end{array} \right) \begin{array}{l} \}3 \\ \}n_R \end{array} \quad (\text{A.11})$$

we can diagonalize matrix M_ν

$$U^T M_\nu U = M_{diag}. \quad (\text{A.12})$$

Thanks to this transformation we obtain simultaneously mixing matrix among weak (ν_M) and physical (N) states

$$N_i = \sum_{j=1}^{3+n_R} U_{ij} \nu_{M_j}. \quad (\text{A.13})$$

Eventually the mass Lagrangian takes a form

$$2L_{mass}^{neutrino} = - \sum_{i=1}^{3+n_R} \bar{N}_i (M_{diag})_{ii} N_i. \quad (\text{A.14})$$

Mass matrix for charged leptons m^l is diagonalized by unitary matrix U_L^l

$$L^{leptons} = - \sum_{l=1}^3 m_{diag}^l \bar{\hat{l}} \hat{l}, \quad (\text{A.15})$$

where

$$\hat{l} = U_L^l l. \quad (\text{A.16})$$

LR model

This model is based on the $SU(2)_L \otimes SU(2)_R \otimes U(1)_{B-L}$ gauge group. Lepton sector is the reflection of this symmetry. The left and right lepton (and

quark) states are included in doublets (the quantum numbers connected with $SU(2)_L$, $SU(2)_R$ and $U(1)$ gauge groups, (T_{3L}, T_{3R}, Y) respectively, are included in brackets)

$$\Psi_{iL} = \begin{pmatrix} \nu_i \\ l_i^- \end{pmatrix}_L : (2, 1, -1), \quad \Psi_{iR} = \begin{pmatrix} \nu_i \\ l_i^- \end{pmatrix}_R : (1, 2, -1) \quad (\text{A.17})$$

where index i for neutrinos and l_i for leptons stand for e, μ, τ .

Higgs sector can be realized on many ways in this model [64]. Classical model [65] which I use here includes a bidoublet and two triplets

$$\phi = \begin{pmatrix} \phi_1^0 & \phi_1^+ \\ \phi_2^- & \phi_2^0 \end{pmatrix}, \quad (\text{A.18})$$

$$\Delta_{L,R} = \begin{pmatrix} \delta_{L,R}^+/\sqrt{2} & \delta_{L,R}^{++} \\ \delta_{L,R}^0 & -\delta_{L,R}^+/\sqrt{2} \end{pmatrix}. \quad (\text{A.19})$$

Spontaneous symmetry breaking mechanism minimalizes Higgs potential for the following choice of the vacuum expectation values of the $\delta_{R,L}^0$, $\phi_{1,2}^0$ fields [65]

$$\langle \Phi \rangle = \begin{pmatrix} \kappa_1/\sqrt{2} & 0 \\ 0 & \kappa_2/\sqrt{2} \end{pmatrix}, \quad \langle \Delta_{L,R} \rangle = \begin{pmatrix} 0 & 0 \\ v_{L,R}/\sqrt{2} & 0 \end{pmatrix}. \quad (\text{A.20})$$

In this model the lepton part of the Lagrangian allowed by gauge symmetry takes the form

$$\begin{aligned} L_{leptons} \equiv & L_Y^B + L_Y^L + L_Y^R = i\bar{\Psi}_L D\Psi_L + i\bar{\Psi}_R D\Psi_R - \bar{\Psi}_L [h\phi + \tilde{h}\tilde{\phi}] \Psi_R \\ & - \bar{\Psi}_L C i\tau_2 h_L \Delta_L \Psi_L - \bar{\Psi}_R C i\tau_2 h_R \Delta_R \Psi_R \end{aligned} \quad (\text{A.21})$$

where

$$\tilde{\phi} = \tau_2 \phi^* \tau_2,$$

$D = \gamma^\mu D_\mu$ and D_μ equals

$$D_\mu = \begin{cases} \partial_\mu - ig\frac{\vec{\tau}}{2}\vec{W}_{L\mu} + \frac{ig'}{2}YB_\mu & \text{for left spinors} \\ \partial_\mu - ig\frac{\vec{\tau}}{2}\vec{W}_{R\mu} + \frac{ig'}{2}YB_\mu & \text{for right spinors.} \end{cases} \quad (\text{A.22})$$

The left-right symmetry forces the following relations

$$h = h^\dagger \quad , \quad \tilde{h} = \tilde{h}^\dagger \quad , \quad h_L = h_R. \quad (\text{A.23})$$

Let's assume that left triplet does not condensate ($v_L = 0$) - this ensures that unnaturally small values of parameters in Higgs potential are absent. Discussion of necessity (and naturality) for such choice has been carried out in [48], [65]⁹ and then the mass matrix for neutrinos is of the type

$$M_\nu = \begin{pmatrix} \overbrace{0}^3 & \overbrace{m_D}^3 \\ m_D^T & M_R \end{pmatrix} \begin{matrix} \}3 \\ \}3 \end{matrix}. \quad (\text{A.24})$$

where

$$m_D = \frac{1}{\sqrt{2}} (h\kappa_1 + \tilde{h}\kappa_2) \quad \text{and} \quad M_R = \sqrt{2}h_R v_R \quad (\text{A.25})$$

are hermitian and symmetric matrices of dimension 3, respectively. Masses of charged leptons come from the same Yukawa couplings

$$m^l = \frac{1}{\sqrt{2}} (h\kappa_2 + \tilde{h}\kappa_1). \quad (\text{A.26})$$

Similarly to the previous model we can define matrices U, U_L^l which transform weak neutrino and charged lepton states to the physical ones and to get mass matrices as in Eq.(A.14) (with $n_R = 3$) and in Eq.(A.15).

Together we get three light neutrinos and three heavy ones of the order of v_R ($v_R \gg \kappa_1, \kappa_2$).

⁹ The interest is in $\beta_1, \beta_2, \beta_3$ parameters which multiply terms which mix Δ_L fields with Δ_R ones, for instance ([65], (A.2)): $\beta_1 (Tr[\phi \Delta_R \phi^\dagger \Delta_L^\dagger] + Tr[\phi^\dagger \Delta_L \phi \Delta_R^\dagger])$. Consistency between potential minimalization (which gives relation where $v_L \sim \beta_i$) and any allowed spectrum of light neutrino masses (mass matrix for light neutrinos is on the other hand proportional to v_L) demand $\beta_i \leq 10^{-6}$ [65]. Discrete symmetry of the type $\Delta_L \rightarrow \Delta_R, \Delta_R \rightarrow -\Delta_L$ can eliminate this difficulty [48].

7 Appendix B. Couplings of neutrinos in charged and neutral currents. Couplings of neutrinos with Higgs particles

In this Appendix I describe all relevant couplings which must be known for numerical calculations of the considered processes $e^-e^+ \rightarrow N_a N_b$ (Section 3) and $e^-e^- \rightarrow W^-W^-$ (Section 4).

RHS model

Charged and neutral currents have the form as in the SM

$$L_{CC} = \frac{g}{\sqrt{2}} \bar{\nu}_{iL} \gamma^\mu l_{iL} W_\mu^+ + h.c., \quad (\text{B.1})$$

$$L_{NC} = \frac{g}{2 \cos \theta_W} Z_\mu \bar{\nu}_{iL} \gamma^\mu \nu_{iL}. \quad (\text{B.2})$$

These interactions can be written using relations (A.13),(A.16) in a base of physical states

$$L_{CC} = \frac{g}{\sqrt{2}} \bar{N} \gamma^\mu K P_L \hat{l} W_\mu^+ + h.c., \quad (\text{B.3})$$

$$\begin{aligned} L_{NC} &= \frac{g}{2 \cos \theta_W} Z_\mu \sum_{a,b} \bar{N}_a \gamma^\mu P_L \Omega_{ab} N_b \\ &= \frac{g}{2 \cos \theta_W} Z_\mu \frac{1}{\delta_{ab} + 1} \sum_{a \geq b} \bar{N}_a [\gamma^\mu (P_L \Omega - P_R \Omega^*)]_{ab} N_b \end{aligned} \quad (\text{B.4})$$

where I have used the following denotations¹⁰

$$K = U_L^T U_L^l, \quad \Omega = U_L^\dagger U_L. \quad (\text{B.5})$$

Similarly, writing down Yukawa interaction in physical states we get

$$L_{Yukawa}^{D-D} = -\frac{g}{2M_W} \sum_a \{m_a^l (\bar{l}_a l_a H^0 + i \bar{l}_a \gamma_5 l_a \chi^0)\}$$

¹⁰without losing generality the matrix U_L^l can be chosen as the identity one [23] and such approach is used in this Thesis.

$$L_{Yukawa}^{D-M} = -\frac{g}{2M_W} \chi^- \left(\sum_{a,b} \bar{l}_a [P_R (K^\dagger)_{ab} m_b^N - P_L m_a^l (K^\dagger)_{ab}] N_b \right) + h.c. \quad (\text{B.6})$$

for vertices which include two Dirac fermion particles ('Dirac-Dirac' vertex) or one Dirac and one Majorana particles ('Dirac-Majorana' vertex).

For 'Majorana-Majorana' vertices:

$$\begin{aligned} L_{Yukawa}^{M-M}(H^0) &= -\frac{g}{2M_W} H^0 \sum_{a,b} \left(\bar{N}_a \Omega_{ab} m_b^N P_R N_b + \bar{N}_a m_a^N \Omega_{ab} P_L N_b \right) \\ &= -\frac{g}{2M_W} H^0 \frac{1}{\delta_{ab} + 1} \\ &\quad \sum_{a \geq b} \bar{N}_a \left[P_R (\Omega_{ab} m_b^N + \Omega_{ab}^* m_a^N) + P_L (\Omega_{ab} m_a^N + \Omega_{ab}^* m_b^N) \right] N_b \end{aligned} \quad (\text{B.7})$$

$$\begin{aligned} L_{Yukawa}^{M-M}(\chi^0) &= -\frac{ig}{2M_W} \chi^0 \sum_{a,b} \left(\bar{N}_a \Omega_{ab} m_b^N P_R N_b - \bar{N}_a m_a^N \Omega_{ab} P_L N_b \right) \\ &= -\frac{ig}{2M_W} \chi^0 \frac{1}{\delta_{ab} + 1} \\ &\quad \sum_{a \geq b} \bar{N}_a \left[P_R (\Omega_{ab} m_b^N + \Omega_{ab}^* m_a^N) - P_L (\Omega_{ab} m_a^N + \Omega_{ab}^* m_b^N) \right] N_b \end{aligned} \quad (\text{B.8})$$

LR model

This model involves two pairs of charged and neutral gauge bosons. Their masses come from the kinetic part of the Higgs Lagrangian

$$L_{kinet} = Tr(D^\mu \phi)^\dagger (D_\mu \phi) + Tr(D^\mu \Delta_L)^\dagger (D_\mu \Delta_L) + Tr(D^\mu \Delta_R)^\dagger (D_\mu \Delta_R) \quad (\text{B.9})$$

where

$$\begin{aligned}
D^\mu \phi &= \partial_\mu \phi - ig \frac{\vec{\tau}}{2} \phi \vec{W}_{L\mu} + ig \phi \frac{\vec{\tau}}{2} \vec{W}_{R\mu} \\
D^\mu \Delta_{L,R} &= \partial_\mu \Delta_{L,R} - ig \vec{W}_{L,R\mu} \left[\frac{\vec{\tau}}{2}, \Delta_{L,R} \right] - ig' B_\mu \Delta_{L,R}
\end{aligned} \tag{B.10}$$

Writing at length this Lagrangian we obtain after spontaneous symmetry breaking (Eq.(A.20)) mass matrices for gauge fields ($\kappa_+^2 = \kappa_1^2 + \kappa_2^2$)

$$\tilde{M}_W^2 = \frac{g^2}{4} \begin{pmatrix} \kappa_+^2 & -4\kappa_1\kappa_2 \\ -4\kappa_1\kappa_2 & \kappa_+^2 + 2v_R^2 \end{pmatrix}, \tag{B.11}$$

$$\tilde{M}_0^2 = \begin{pmatrix} \frac{g^2}{2}\kappa_+^2 & -\frac{g^2}{2}\kappa_+^2 & 0 \\ -\frac{g^2}{2}\kappa_+^2 & \frac{g^2}{2}(\kappa_+^2 + 4v_R^2) & -4gg'v_R^2 \\ 0 & -4gg'v_R^2 & 4g'^2v_R^2 \end{pmatrix}. \tag{B.12}$$

Let's take unitary matrices which transform weak gauge boson states to physical states in the form

$$\begin{pmatrix} W_1^\pm \\ W_2^\pm \end{pmatrix} = \begin{pmatrix} \cos \zeta & -\sin \zeta \\ \sin \zeta & \cos \zeta \end{pmatrix} \begin{pmatrix} W_L^\pm \\ W_R^\pm \end{pmatrix}, \tag{B.13}$$

for the charged sector and

$$\begin{pmatrix} Z_1 \\ Z_2 \\ A \end{pmatrix} = \begin{pmatrix} c_W c, & -s_W c_M c - s_M s, & -s_W s_M c + c_M s \\ c_W s, & -s_W c_M s + s_M c, & -s_W s_M s - c_M c \\ s_W, & c_W c_M, & c_W s_M \end{pmatrix} \begin{pmatrix} W_{3L} \\ W_{3R} \\ B \end{pmatrix}, \tag{B.14}$$

for the neutral one, where

$$\begin{aligned}
c_W &= \cos \Theta_W, \quad s_W = \sin \Theta_W, \quad c = \cos \phi, \quad s = \sin \phi, \\
c_M &= \tan \Theta_W, \quad s_M = \frac{\sqrt{\cos 2\Theta_W}}{\cos \Theta_W}.
\end{aligned}$$

Transformations (B.13) and (B.14) define two mixing angles ζ, ϕ and masses of gauge bosons which with good approximation are ([48],[66])

$$\zeta \simeq \frac{2\kappa_1\kappa_2}{\kappa_1^2 + \kappa_2^2} \frac{M_{W_1}^2}{M_{W_2}^2}, \quad \phi \simeq -\frac{(\cos 2\Theta_W)^{3/2}}{2 \cos^4 \Theta_W} \frac{M_{W_1}^2}{M_{W_2}^2}$$

$$M_{W_1}^2 \simeq \frac{g^2}{2}(\kappa_1^2 + \kappa_2^2), \quad M_{W_2}^2 \simeq \frac{g^2}{2}v_R^2, \quad (\text{B.15})$$

$$M_{Z_1}^2 \simeq \frac{g^2}{2\cos^2\Theta_W}(\kappa_1^2 + \kappa_2^2), \quad M_{Z_2}^2 \simeq \frac{2g^2\cos^2\Theta_W}{\cos 2\Theta_W}v_R^2. \quad (\text{B.16})$$

Let's note that relations (A.25) with $h_R \leq 1$ and (B.15) gives upper bound on heavy neutrino masses

$$M_N \leq \frac{2M_{W_2}}{g}. \quad (\text{B.17})$$

Using transformations (A.13), (A.16) we can state charged and neutral currents as follows [66]

$$L_{CC} = \frac{g}{\sqrt{2}} \sum_{i=1}^2 \bar{N} \gamma^\mu [A_L^{(i)} P_L + A_R^{(i)} P_R] \hat{W}_{i\mu}^+ + h.c., \quad (\text{B.18})$$

and

$$L_{NC}^{D-D} = \frac{g}{2\cos\Theta_W} \sum_{i=1}^2 \bar{l} \gamma^\mu [A_L^{il} P_L + A_R^{il} P_R] \hat{Z}_{i\mu} \quad (\text{B.19})$$

for ‘Dirac-Dirac’ vertex. For ‘Majorana-Majorana’ ones we have

$$\begin{aligned} L_{NC}^{M-M} &= \frac{g}{2\cos\Theta_W} Z_{i\mu} \sum_{a,b} \bar{N}_a \gamma^\mu (P_L(\Omega_L)_{ab} A_L^{i\nu} + P_R(\Omega_R)_{ab} A_R^{i\nu}) N_b \\ &= \frac{g}{2\cos\Theta_W} Z_{i\mu} \frac{1}{\delta_{ab} + 1} \\ &\quad \times \sum_{a \geq b} \bar{N}_a \gamma^\mu [(A_L^{i\nu} + A_R^{i\nu})(P_L(\Omega_L)_{ab} - P_R(\Omega_L)_{ab}^*) + (P_R - P_L) A_R^{i\nu} \delta_{ab}] N_b \end{aligned} \quad (\text{B.20})$$

where (a stands for leptons (a=e,μ,τ) and β stands for neutrinos (β = 1, ..., 6))

$$\begin{aligned} (A_L^{(1)})_{a\beta} &= \cos \xi (K_L)_{a\beta}, & (A_R^{(1)})_{a\beta} &= -\sin \xi (K_R)_{a\beta}, \\ (A_L^{(2)})_{a\beta} &= \sin \xi (K_L)_{a\beta}, & (A_R^{(2)})_{a\beta} &= \cos \xi (K_R)_{a\beta}, \end{aligned} \quad (\text{B.21})$$

and

$$A_{L(R)}^{il(\nu)} = g_{L(R)}^{il(\nu)} \cos \phi + g'_{L(R)}{}^{il(\nu)} \sin \phi,$$

$$g_L^{1l} = g_L^{2l} = -1 + 2 \sin^2 \Theta_W \quad (\text{B.22})$$

$$g_L^{1l} = -g_L^{2l} = g_L^{1\nu} = -g_L^{2\nu} = -\frac{\sin^2 \Theta_W}{\sqrt{\cos 2\Theta_W}} \quad (\text{B.23})$$

$$g_L^{1\nu} = g_L^{2\nu} = 1 \quad g_R^{1\nu} = g_R^{2\nu} = 0 \quad (\text{B.24})$$

$$g_R^{1l} = g_R^{2l} = 2 \sin^2 \Theta_W \quad (\text{B.25})$$

$$g_R^{1l} = -g_R^{2l} = -\frac{1 - 3 \sin^2 \Theta_W}{\sqrt{\cos 2\Theta_W}} \quad (\text{B.26})$$

$$g_R^{1\nu} = -g_R^{2\nu} = -\frac{\cos^2 \Theta_W}{\sqrt{\cos 2\Theta_W}} \quad (\text{B.27})$$

Let's note that the neutral part of this Lagrangian for charged leptons conserves the lepton flavour. Mixing matrices $K_{L,R}$ and $\Omega_{L,R}$ have 6×3 , 6×6 dimensions, respectively and are connected with transformation of fields to physical states¹¹

$$K_L \equiv K = U_L^\dagger U_L^l, \quad K_R = U_R^\dagger U_R^l, \quad \Omega_L \equiv \Omega = U_L^\dagger U_L, \quad \Omega_R = U_R^\dagger U_R. \quad (\text{B.28})$$

In the paper I consider the influence of the LR model's Higgs sector on the $e^+e^- \rightarrow \nu N$ cross section. The value of this cross section depends both on the Higgs bosons masses and on their couplings with leptons. The form of the Higgs potential from which Higgs particles' masses can be obtained is large. Full discussion of the Higgs potential diagonalization and their couplings with neutrinos have been performed in [48] and [65]. I will restrict here only to showing indispensable relations for $e^+e^- \rightarrow \nu N$ analysis.

¹¹Similarly to the RHS model (Eq.(B.5)) we can choose charged lepton mixing matrices $U_{L,R}^l$ as identity. We denote matrices K_L and Ω_L which enter in left-handed currents exactly as in the RHS model to make discussion of their meaning common through this Thesis (Sections 3 and 4).

Higgs fields give altogether 20 degrees of freedom. Minimalization of the Higgs potential gives 16 different particles (denotations according to [48]):

- 4 Goldstone' bosons ($G_{L,R}^{\pm}, G_{L,R}^0$),
- 6 neutral Higgs bosons ($H_0^0, H_1^0, H_2^0, H_3^0, A_1^0, A_2^0$),
- 2 single charged particles (H_1^{\pm}, H_2^{\pm}),
- 2 doubly charged particles ($\delta_{L,R}^{\pm\pm}$).

Considering the existing experimental data it is justified to assume that

$$v_R \gg y = \sqrt{\kappa_1^2 + \kappa_2^2} \quad (\text{B.29})$$

and, taking into account energies for which we make investigations, $\sqrt{s} \gg m_e \simeq 0$. Then it turns out that only two neutral Higgs particles H_1^0, A_1^0 and two charged ones H_1^{\pm}, H_2^{\pm} have nonzero couplings with leptons (Fig.2). Masses of these particles are

$$\begin{aligned} M_{H_1^{\pm}}^2 &= \frac{1}{2} \left[v_R^2 + \frac{1}{2} y^2 \sqrt{1 - \epsilon^2} \right], \\ M_{H_2^{\pm}}^2 &= \frac{1}{2} \left[v_R^2 \frac{1}{\sqrt{1 - \epsilon^2}} + \frac{1}{2} y^2 \sqrt{1 - \epsilon^2} \right], \\ M_{H_1^0}^2 &\simeq \frac{1}{2} v_R^2 \frac{1}{\sqrt{1 - \epsilon^2}}, \\ M_{A_1^0}^2 &\simeq \frac{1}{2} \left[v_R^2 \frac{1}{\sqrt{1 - \epsilon^2}} - 4y^2 \right] \end{aligned} \quad (\text{B.30})$$

where

$$0 \leq \epsilon = \frac{2\kappa_1\kappa_2}{\kappa_1^2 + \kappa_2^2} \leq 1.$$

Their couplings with leptons (Eq.(A.21) are (symbols $\Gamma^{(x)}$, $x=1N,1,N$ are taken from Appendix C)

- H_1^\pm , exchange ($X \equiv K^\dagger K_R^T M_{diag}^\nu K_R K^*$)

$$\begin{aligned}\Gamma_{lN} (H_1^\pm)_{N_b e^-} &= \frac{1}{v_R} \sum_{c=4,5,6} X_{bc} (K)_{ce} P_L, \\ \Gamma_{lN} (H_1^\pm)_{e^+ N_a} &= \frac{1}{v_R} \sum_{c=4,5,6} (K^\dagger)_{ec} (X^*)_{ca} P_R.\end{aligned}\quad (\text{B.31})$$

- H_2^\pm , exchange ($\alpha_2 = \frac{\sqrt{2}}{y\sqrt{1-\epsilon^2}}$).

$$\begin{aligned}\Gamma_{lN} (H_2^\pm)_{N_b e^-} &= - [m_b^N (K)_{be} \epsilon \alpha_2] P_L + \\ &\left[- \sum_{c=4,5,6} (\Omega_L)_{bc} m_c^N (K_R)_{ce} \alpha_2 + \frac{1}{\alpha_2 v_R^2} \sum_{c=4,5,6} (\Omega_R^*)_{bc} m_c^N (K_R)_{ce} \right] P_R,\end{aligned}\quad (\text{B.32})$$

$$\begin{aligned}\Gamma_{lN} (H_2^\pm)_{e^+ N_a} &= - [(K^\dagger)_{ea} m_a^N \epsilon \alpha_2] P_R + \\ &\left[- \sum_{c=4,5,6} (K_R^\dagger)_{ec} m_c^N (\Omega)_{ca} \alpha_2 + \frac{1}{\alpha_2 v_R^2} \sum_{c=4,5,6} (K_R^\dagger)_{ec} m_c^N (\Omega_R^*)_{ca} \right] P_L.\end{aligned}\quad (\text{B.33})$$

- neutral particles' exchange H_0^0, H_1^0 and A_1^0

Let's denote

$$\begin{aligned}A_0 &\simeq \frac{1}{y\sqrt{1-\epsilon^2}} [H_1^0 - iA_1^0], \\ B_0 &\simeq \frac{1}{y} H_0^0 - \frac{\epsilon}{y\sqrt{1-\epsilon^2}} [H_1^0 + iA_1^0],\end{aligned}\quad (\text{B.34})$$

then couplings ($e^- e^+ H$) and ($N_a N_b H$) can be written in the form

$$\begin{aligned}\Gamma_l (\{\mathbf{H}_0^0\}, H_1^0, A_1^0)_{e^- e^+} &= - \left[\sum_{c=4,5,6} (K^\dagger)_{ce} (K_R)_{ce} m_c^N A_0 \right] P_R \\ &- \left[\sum_{c=4,5,6} (K^*)_{ce} (K_R^*)_{ce} m_c^N A_0^* \right] P_L,\end{aligned}\quad (\text{B.35})$$

(let's note that the lightest Higgs particle H_0^0 does not couple with e^-e^+ pair if we neglect the mass of electron)

$$\begin{aligned}
\left[\Gamma_N + \Gamma_N^C\right]_{N_a N_b} (H_0^0, H_1^0, A_1^0) = & - [((\Omega)_{ba} m_a^N + (\Omega)_{ab} m_b^N) B_0 \\
& + \sum_{l=\mu,\tau} m_l ((K)_{bl} (K_R^*)_{al} + (K)_{al} (K_R^*)_{bl}) A_0^*] P_R \\
& - [((\Omega)_{ba}^* m_a^N + (\Omega)_{ba} m_b^N) B_0^* \\
& + \sum_{l=\mu,\tau} m_l ((K^*)_{bl} (K_R)_{al} + (K^*)_{al} (K_R)_{bl}) A_0] P_L.
\end{aligned}
\tag{B.36}$$

8 Appendix C. Feynman rules for Majorana neutrino interactions

Majorana neutrinos are self-conjugate spin one half fields. Their self-conjugacy is responsible for the existence of four different propagators in contrary to the Dirac neutrino case where only one propagator exists. This property gives also bigger number of vertices and the problem with establishing relative signatures of various diagrams contributing to a given amplitude. We can however, similarly to the Dirac case, introduce the Feynman diagram technique which in a consistent way describes Majorana particles both for charged and neutral currents.

Let's define a general form of Majorana particle interactions with gauge fields in the following way (N - Majorana neutrino, l - charged lepton, W^\pm, Z^0 - gauge bosons)

$$L_{CC} = \bar{N}\Gamma_l^\mu l W_\mu^+ + \bar{l}\bar{\Gamma}_l^\mu N W_\mu^- \quad (C.1)$$

$$\begin{aligned} L_{NC} &= \bar{l}\Gamma_{lN}^\mu l Z_\mu^0 + \bar{N}\bar{\Gamma}_N^\mu N Z_\mu^0 = \bar{l}\Gamma_{lN}^\mu l Z_\mu^0 + Z_\mu^0 \sum_{a,b} \bar{N}_a (\Gamma_N^\mu)_{ab} N_b \\ &= \bar{l}\Gamma_{lN}^\mu l Z_\mu^0 + Z_\mu^0 \frac{1}{\delta_{ab} + 1} \left(\sum_{a \geq b} \bar{N}_a (\Gamma_N^\mu)_{ab} N_b + \bar{N}_b (\Gamma_N^\mu)_{ba} N_a \right) \\ &= \bar{l}\Gamma_{lN}^\mu l Z_\mu^0 + Z_\mu^0 \frac{1}{\delta_{ab} + 1} \left(\sum_{a \geq b} \bar{N}_a [\Gamma_N^\mu + \Gamma_N^{\mu C}]_{ab} N_b \right) \end{aligned} \quad (C.2)$$

where

$$\Gamma_{(x)}^\mu = \gamma^\mu \left(P_L A_L^{(x)} + P_R A_R^{(x)} \right), \quad x = l, N, lN, \quad (C.3)$$

$$\bar{\Gamma}_l^\mu = \gamma_0 \Gamma_l^{\mu\dagger} \gamma_0 \quad (C.4)$$

and

$$\Gamma_N^{\mu C} = C \Gamma_N^{\mu T} C^{-1}. \quad (C.5)$$

Making algebraic manipulations in Eq.(C.2) we have used self-conjugacy of Majorana field ($N^C \equiv C\bar{N}^T = N$). Similarly, let's define Majorana particle - Higgs boson (H^\pm, H^0) interaction

$$L_{NH^\pm} = \bar{N}\Gamma_l l H^+ + \bar{l}\bar{\Gamma}_l N H^- \quad (\text{C.6})$$

$$\begin{aligned} L_{NH^0} &= \bar{l}\Gamma_{lN} l H^0 + \bar{N}\bar{\Gamma}_N N H^0 = \bar{l}\Gamma_{lN} l H^0 + H^0 \sum_{a,b} \bar{N}_a (\Gamma_N)_{ab} N_b \\ &= \bar{l}\Gamma_{lN} l H^0 + H^0 \frac{1}{\delta_{ab} + 1} \left(\sum_{a \geq b} \bar{N}_a (\Gamma_N)_{ab} N_b + \bar{N}_b (\Gamma_N)_{ba} N_a \right) \\ &= \bar{l}\Gamma_{lN} l H^0 + H^0 \frac{1}{\delta_{ab} + 1} \left(\sum_{a \geq b} \bar{N}_a [(\Gamma_N) + (\Gamma_N)^C]_{ab} N_b \right) \end{aligned} \quad (\text{C.7})$$

where

$$\Gamma_{(x)} = \left(P_L B_L^{(x)} + P_R B_R^{(x)} \right), \quad x = l, N, lN, \quad (\text{C.8})$$

$$\bar{\Gamma}_l = \gamma_0 \Gamma_l^\dagger \gamma_0 \quad (\text{C.9})$$

and

$$\Gamma_N^C = C \Gamma_N^T C^{-1}. \quad (\text{C.10})$$

Two remarks are necessary. Firstly, we would like to read out a form of appropriate vertices for Majorana particles directly from Lagrangian as is in the case of Dirac fermions both in QED and QCD. The above form of the Lagrangian satisfies this demand, for instance, the contents of the rectangle brackets in Eqs.(C.2),(C.7) describe Majorana-Majorana-boson vertices (up to the i factor). Secondly, I consider two non-standard models in this Thesis. In the previous Appendices I have written down the Lagrangian and/or couplings of particles in these models I need through the Thesis, in agreement with the above denotations, so vertices can be easily read from them.

Let's proceed to Feynman rules for any process involving Majorana particles. These rules are based on the following procedure that we should

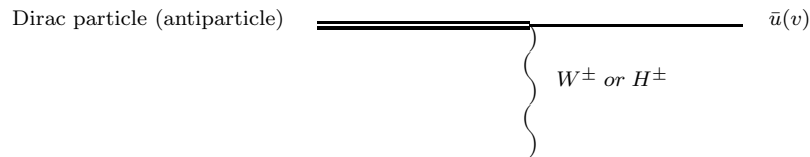
perform:

- (i) attribute spinors to fermion lines on the given Feynman diagram (not only to external lines);
- (ii) set up a form of vertices;
- (iii) build up a propagator in the way to get a Dirac type one;
- (iv) establish related sign between different diagrams.

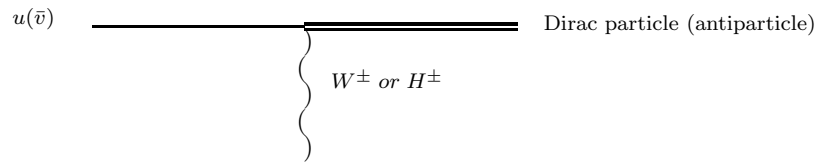
Ad.(i): Spinors

For the Majorana-charged lepton coupling with charged gauge (Higgs) bosons (let's call it 'Majorana-Dirac' coupling) the spinors' attribution to the Majorana line depends on the nature of the Dirac line

(a) For incoming Dirac particle (antiparticle) the outgoing Majorana fermion must be treated as a particle (antiparticle)

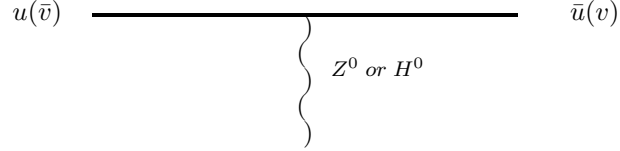


(b) For outgoing Dirac particle (antiparticle) the incoming Majorana fermion must be treated as a particle (antiparticle)



We can see that for the Dirac-Majorana transition the attribution of spinors to Majorana lines is definitive. This is not the case for neutral

Majorana-Majorana -neutral boson couplings (let's call it 'Majorana-Majorana' couplings). Here we can treat a Majorana fermion as a particle or an antiparticle



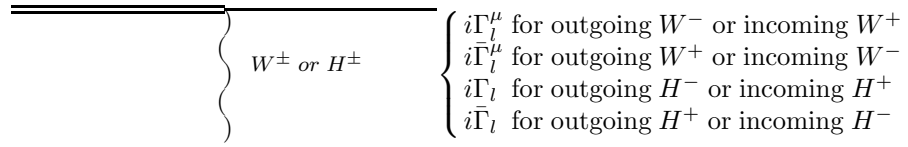
If the 'fermion flow' on the diagram is opposite to the momentum flow then we can use the relation

$$u(\pm k) = v(\mp k)$$

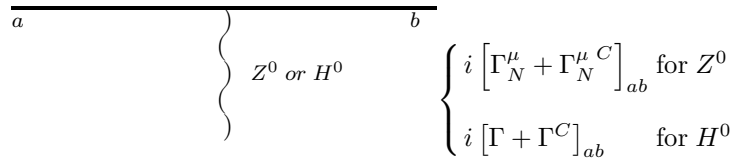
to change its direction.

Ad.(ii) Vertices

(a) For a Dirac-Majorana coupling with a charged boson we have



(b) For a Majorana-Majorana coupling with a neutral boson we have



Ad.(iii) Propagators

We build up an amplitude in a way to get only one type of propagator for a virtual Majorana particle, the same as for the Dirac case which we build from u-type spinors

$$u(k)\bar{u}(k) \rightarrow i \sum_{spin(\lambda)} \frac{u(\vec{k}, \lambda)\bar{u}(\vec{k}, \lambda)}{k^2 - m^2 + i\epsilon} = \frac{i(\hat{k} + m)}{k^2 - m^2 + i\epsilon} \equiv iS(k)$$

To do it we may sometimes need useful relations between spinors

$$\bar{v}_b O u_a = \bar{v}_a O^C u_b; \quad \bar{u}_b O u_a = \bar{u}_a O^C u_b \quad (\text{C.11})$$

where $O = (\Gamma^\mu, \Gamma)$ and $O^C = CO^T C^{-1}$.

If both (Majorana) spinors a and b describe external particles we have to take relations (C.11) with the minus sign.

Ad.(iv): Sign convention

The amplitude is used to calculate the cross section so we need to know only a relative sign between various diagrams. This relative sign can be established as follows:

- choose any Feynman diagram which we call a reference diagram. In this diagram fermions appear in a given order;
- compare all the other diagrams with the reference one. Permute fermions in their ‘fermion chain’ to get the same order as in the reference one;
- if parity of the permutation is odd (even) then we change (unchange) signature of the amplitude.

Examples can be found in [67] (see also [68]). These rules can be applied to loops diagrams, too ([67],[69]).

References

- [1] S. Weinberg, Phys.Rev.Lett.**19**(1967)1264; A. Salam, in Elementary Particle Physics, ed. N. Svartholm (Almqvist and Wiksells, Stockholm, 1968), p.367; S. Glashow, J. Iliopoulos and L. Maiani, Phys.Rev.**D2**(1970)1285; D. Gross and F. Wilczek, Phys.Rev. **D8** (1973)3633; S. Weinberg, Phys.Rev.Lett.**31**(1973)494; H. Fritzsch, M. Gell-Mann and H. Leutwyler, Phys.Lett.**B365**(1973)365; D. Gross and F. Wilczek, Phys.Rev.Lett.**30**(1973)1343; H.D. Politzer, Phys.Rev.Lett. **30**(1973)1346.
- [2] S.L. Glashow Rev.Mod.Phys. **52**(1980)539.
- [3] S. Pokorski ‘Status of the electroweak interactions: theoretical aspects’, ICHEP, Warsaw 1996.
- [4] C. Athanassopoulos, et.al, Phys.Rev.Lett.**75**(1995)2650; *ibid.* **77**(1996)3082.
- [5] J. Ellis in ‘Testing the Standard Model and beyond’, CERN-TH/95-317 (hep-th/9512133) and references therein.
- [6] Proc. of the Workshop on physics and experiments with linear colliders (Saariselkä, Finland, September 1991), edited by R. Orava, P. Eerola and M. Nordberg (World Scientific, 1992) and Proc. of the Workshop on physics and experiments with linear colliders (Waikoloa, Hawaii, April 1993), edited by F.A. Harris, S.L. Olsen, S. Pakvasa and X. Tata (World Scientific, 1993); Proc. of the Electron-Electron Linear Collider Workshop e^-e^- , Int.J.Mod. Phys.**A11**,No.9(1996) edited by C.A. Heusch.

- [7] Physics and Technology of the Next Linear Collider: a report submitted to Snowmass '96 by NLC ZDR Design Group and NLC Physics Working Group (S. Kuhlman et al.), hep-ex/9605011.
- [8] see [7], also F. Cuypers, hep-ph/9512201.
- [9] J. Gluza and M. Zralek, Acta Phys. Pol. **B27**(1996)1557.
- [10] B.W. Lee and R. Shrock, Phys.Rev.**D16**(1977)1444; B.W. Lee; S. Pakvasa, R. Shrock and H. Sugawara Phys.Rev.Lett.38(1977)937; W. Marciano and I. Sanda, Phys.Lett.**B37**(1977)303.
- [11] T.P. Cheng and L.F. Li, Phys.Rev.**D44**(1991)1502, A. Ilakovac and A. Pilaftsis Nucl.Phys.**B437**(1995)491; D. Tommasini, G. Barenboim, J. Bernabeu and C. Jarlskog, Nucl. Phys. **B444** (1995) 451; R.N. Mohapatra and J.W.F. Valle, Phys. Rev. **D34** (1986) 1642; E. Witten, Nucl. Phys. **B268** (1986) 79; J. Bernabeu et al., Phys. Lett. **B187** (1987) 303; J.L. Hewett and T.G. Rizzo, Phys. Rep. **183** (1989) 193; E. Nardi, Phys. Rev. **D48** (1993) 3277.
- [12] P. Langacker, D. London Phys.Rev.**D38**(1988)886; E. Nardi, E. Roulet, D. Tommasini Nucl.Phys.**B386**(1992)239; Phys.Lett.**B344** (1995)225, C.P. Burgess et.al Phys.Rev.**D49**(1994)6115.
- [13] C. Jarlskog, Phys.Lett. **B241**(1990)579; S.M. Bilenky, W. Grimus, H. Neufeld, Phys.Lett. **B252**(1990)119; C.O. Escobar et al., Phys.Rev. **D47**(1993)R1747;
- [14] W. Keung, G. Senjanovic, Phys.Rev.Lett. **50**(1983)1427; D.A. Dicus, D.D. Karatas, P. Roy, Phys.Rev. **D44**(1991)2033; B. Mukhopadhyaya, Phys.Rev. **D49**(1994)1350, H. Tso-hsiu, Ch. Cheng-rui,

- T. Zhi-jian, Phys.Rev.**D42**(1990)2265; A. Datta, M. Guchait, D.P. Roy Phys.Rev.**D47**(1993)961; D.A. Dicus, P. Roy, Phys.Rev. **D44**(1991)1593.
- [15] A. Djouadi, J. Ng, T.G. Rizzo ‘New particles and interactions’ hep-ph/9504210.
- [16] S.M. Bilenky, C. Giunti Phys.Lett.**B300**(1993)137.
- [17] Particle Data Group, Phys. Rev. **D54**(1996) Part 1, p.280; K. Assamagan et.al., Phys. Rev. **D53**(1996)6065; D. Buskulic et.al., Phys.Lett. **B349**(1995)585.
- [18] L3 Collab., B. Adeva et.al., Phys.Lett.**B251**(1990)321.
- [19] L3 Collab., O.Adriani et al., Phys. Letters B 295(1992)371.
- [20] J.C. Pati and A. Salam, Phys.Rev.**D10**(1974)275; R.N. Mohapatra and J.C. Pati,ibid.**D11**(1975)566;**D11**(1975)2559; G. Senjanovic and R.N. Mohapatra,ibid.**D12**(1975)152; G. Senjanovic, Nucl.Phys.**B153**(1979)334.
- [21] A. Jodidio et.al.,Phys.Rev.**D34**(1986)1967.
- [22] F. Abe et.al.,Phys.Rev.Lett.**74**(1995)2900.
- [23] S.M. Bilenky and S.T. Petcov, Review of Mod.Phys. **59**(1987)671.
- [24] P. Minkowski, Waikoloa Linear Collid.(1993)524 (QCD183:I795:1993).
- [25] D. Wyler and L. Wolfenstein, Nucl. Phys. **B218** (1983) 205.
- [26] G. Belanger, F. Boudjema, D. London and H. Nadeau, Phys.Rev.**D53**(1996)6292.

- [27] J. Gluza, J. Maalampi, M. Raidal and M. Zralek, ‘Mixings of heavy neutrinos and their production at Linear Collider’, in preparation.
- [28] T. Yanagida, Proc. of the Workshop on Unified Theory and Baryon Number in the Universe, eds. O. Sawada and A. Sugamoto (KEK,1979), M. Gell-Mann, P. Ramond and R. Slansky, in Supergravity, ed.by P. Van Nieuwenhuizen and D. Freedman (North-Holland,Amsterdam,1979).
- [29] B. Armbruster et.al., Phys.Lett.**B348**(1995)19.
- [30] M.M. Guzzo, O.L.G. Peres, V. Pleitez and R. Zukanovich Funchal, Phys.Rev.**D53** (1996)2851.
- [31] G. Gelmini and E. Roulet, Rep.Prog.Phys. **58**(1995)1207 and references therein.
- [32] G. Ingelman, J. Rathsman Z.Phys.**C60**(1993)243.
- [33] W. Buchmuller, C. Greub Nucl.Phys.**B363**(1991)345, **B381**(1992)109.
- [34] R.N. Mohapatra, P.B. Pal, ”Massive neutrinos in physics and astrophysics”, World Scientific, 1991.
- [35] L.N. Chang, D. Ng and J.N. Ng, Phys. Rev. **D50** (1994) 4589.
- [36] H.B. Thacker and J.J. Sakurai, Phys.Lett.**B36**(1971)103, Y.S. Tsai, Phys.Rev.**D4**(1971)2821; J.D. Bjorken and C.H. Llewellyn Smith, Phys. Rev. **D7**(1973)887; R. Schrock, Phys.Lett.**B96**(1980) 159; Phys.Rev.**D24**(1981)1232 and ibid. (1981)1275; see also Review of Particles Physics, Phys.Rev.**D54**(1996)275; M. Gronau, C.N. Leung, J.L. Rosner Phys.Rev.**D29**(1984)2539.

- [37] see e.g. E. Nardi et al. in [12].
- [38] A. Balysh et al. (Heidelberg-Moscow Coll.), Phys.Lett.**B356**(1995)450.
- [39] see e.g. J.D. Vergados, Phys.Rev. **D28**(1983)2887; Phys.Rep. **133**(1986)1; A. Tomada, Rep.Prog.Phys. **54**(1991)1.
- [40] T. Bernatowicz et.al., Phys.Rev.Lett. **69**(1992)2341; see also [38].
- [41] M. Hirsch, H.V. Klapdor-Kleingrothaus and O. Panella, Phys.Lett. **B374**(1996)7.
- [42] C.A. Heusch, P. Minkowski, hep-ph/9611353.
- [43] J. Gluza and M. Zralek Phys.Lett.**B362**(1995)148.
- [44] A. Pilaftsis, Z.Phys.**C55**(1992)275.
- [45] G. Beall, M. Bander and A. Soni Phys.Rev.Lett. **48**,848(1982).
- [46] G. Ecker, W. Grimus and H. Newfeld, Phys.Lett. **B127** (1983)305; R.N. Mohapatra, G. Senjanovic and M.D. Tran, Phys.Rev. **D28**(1983)546; F.J. Gilman and M.H. Reno, *ibid.***29**(1984)937; F.I. Olness and M.E. Ebel Phys.Rev. **D30**(1984)1034.
- [47] J. Gunion, A. Mendez, F. Olness, Int.Journ.Mod.Phys.**A4**(1987)1085.
- [48] J. Gluza and M. Zralek, Phys. Rev. **D51** (1995) 4695.
- [49] C. Jarlskog and A. Kleppe, Nucl.Phys.**B286**(1987)245; C.H. Albright, C. Jarlskog and B.A. Lindholm, Phys.Rev.**D38**(1988)872; J. Bernabeu, G.C.Branco and M. Gronau, Phys.Lett.**B169Z**(1986)243; G.C. Branco, CERN-TH 7176/94.

- [50] M. Kobayashi, T. Maskawa, Prog.Theor.Phys. **49** (1973) 652.
- [51] G.C. Branco and M. Rabelo, Phys.Lett.**B173**(1986)313; J. Bernabeu et.al., ibid.**B169**(1986)243.
- [52] F.del Aguila and M. Zralek, Nucl.Phys.**B447**(1995)211.
- [53] S.Petcov Phys.Lett.**139B** (1984)421 and **B178**(1986)57.
- [54] J. Gluza, M. Zralek, hep-ph/9612227.
- [55] T. Rizzo, Phys.Lett.**B116** (1982)23.
- [56] D. London, G. Belanger and J.N. Ng, Phys.Lett. **B188** (1987)155; J. Maalampi, A. Pietila and J. Vuori, Nucl.Phys. **B381** (1992)544; C.A. Heusch and P. Minkowski, Nucl. Phys. **B416** (1994) 3 and Phys.Lett.**B374**(1996)116; P. Helde, K. Huitu, J. Maalampi, M. Raidal, Nucl.Phys. **B437** (1995)305; T. Rizzo Int. J. Mod. Phys. **A11**(1996)1563.
- [57] J. Gluza and M. Zralek, Phys. Rev. **D52** (1995) 6238.
- [58] J. Maalampi, A. Pietila and J. Vuori, Phys.Lett. **B297**(1992)327.
- [59] C. Ryan, S. Okubo, Suppl. Nuovo Cim. **11**(1964)234; B. Kayser, F. Gibrat-Debu, F. Perrier, ‘The physics of massive neutrinos’, World Scientific, Singapore 1989; B. Kayser, Phys.Rev.**D26**(1982)1662.
- [60] J. Gluza ‘Doubly charged Higgs particles in the $e^-e^- \rightarrow W^-W^-$ process’, in preparation.
- [61] F. Cuypers, K. Kołodziej, O. Korakianitis and R. Rühl Phys.Lett. **B325**(1994)243.

- [62] J.F.Gunion and A.Tofghi-Niaki, Phys.Rev.**D36**,2671(1987) and **D38**,1433(1988).
- [63] see C.A. Heusch and P. Minkowski in [56].
- [64] D. Chang, R.N. Mohapatra, Phys.Rev.Lett. **58**(1987)1600; R.N. Mohapatra, Phys.Lett. **B198**(1987)69; P. Ramond and D.B. Reiss, Phys.Lett. **B80**(1978)87; K.S. Babu, V.S. Mathur, Phys.Rev. **D38**(1988)3550; S. Bartolini and J. Liu, Nucl.Phys. **B297**(1988)401; S. Rajpoot, Phys.Lett. **B191** (1987)122; A. Davidson and K.C. Wali, Phys.Rev.Lett. **59**(1987)393; B.S. Balakrishna, Phys.Rev.Lett. **60**(1988)1602; K.S. Babu and R.N. Mohapatra, Phys.Rev.Lett. **62**(1989)1079; R.N. Mohapatra, Phys.Lett. **B201**(1988)517; B.S. Balakrishna, A. Kagan and R.N. Mohapatra, Phys.Lett. **B205**(1988)345; B.S. Balakrishna, Phys.Lett. **B214**(1988)267; E. Ma, Phys.Rev.Lett. **63**(1989)1042; B.S. Balakrishna and R.N. Mohapatra, Phys.Lett. **B216**(1989)349.
- [65] J.F.Gunion et.al., Phys.Rev.**D40**(1989)1546; N.G.Deshpande et.al., Phys.Rev.**D44**(1991)837.
- [66] J. Gluza and M. Zrałek, Phys.Rev.**D48**(1993)5093.
- [67] J. Gluza and M. Zrałek, Phys.Rev. **D45**(1992)1693.
- [68] A. Denner et.al., Phys.Lett. **B219**(1992)278; Nucl.Phys. **B387**(1992)467.
- [69] V.M. Dubovik and V.E. Kuznetsov, hep-ph/9606258.